

# Rate Constants for the Quenching of Excited States of Metal Complexes in Fluid Solution

**Morton Z. Hoffman**

*Department of Chemistry, Boston University, Boston, MA 02215, U.S.A.*

**Fabrizio Bolletta and Luca Moggi**

*Department of Chemistry "G. Ciamician", University of Bologna,  
40126 Bologna, Italy*

**Gordon L. Hug**

*Radiation Chemistry Data Center, Radiation Laboratory,  
University of Notre Dame, Notre Dame, IN 46556, U.S.A.*

The rate constants for the quenching of the excited states of metal ions and complexes in homogeneous fluid solution are reported in this compilation. Values of  $k_q$  for dynamic, collisional processes between excited species and quenchers have been critically evaluated, and are presented with the following information, among others, from the original publications, when available: description of the solution medium, temperature at which  $k_q$  was determined, experimental method, range of quencher concentration used, lifetime of the excited state in the absence of quencher, activation parameters, quenching mechanism. Data collection is complete through the end of 1986, and covers the coordination compounds of twenty-six metals, including the ions and complexes of the inner- and outer-transition metals, and porphyrin complexes of non-transition metals. Data for 261 excited states quenched by more than 400 inorganic quenchers and 600 organic quenchers have been extracted from almost 500 publications. The introduction to the work contains a discussion of the conceptual background to quenching, including a general treatment of the kinetics, an explanation of the tables, and a list of recent review articles. Uncommon kinetics mechanisms and equations, used to obtain the reported values of  $k_q$ , are discussed in detail as part of the notes to the tables. Indexes of excited states, quenchers, and authors are appended.

## Contents

1. Introduction .....	3	2.6.e. Partially Unquenchable Reactions ...	9
2. Conceptual Background .....	3	2.6.f. Quenching of a Higher-Energy Excited State .....	9
2.1. Excitation of Substrates .....	3	2.6.g. Static Quenching .....	9
2.2. Decay of Excited States .....	4	2.7. Correction of $k_q$ for Diffusion .....	10
2.3. Quenching of Excited States .....	4	2.8. Cage Escape Efficiency .....	10
2.4. Types of Quenching Processes .....	5	3. Explanation of the Tables .....	11
2.5. Fundamental Quenching Kinetics .....	6	3.1. Scope of the Compilation .....	11
2.6. Other Considerations of the Kinetics .....	8	3.2. Procedures of Selection .....	11
2.6.a. Effects of Ionic Strength .....	8	3.3. Nomenclature and Speciation .....	11
2.6.b. Multiple Forms of the Quencher .....	9	3.4. Errors and Uncertainties .....	12
2.6.c. Non-selective Measurements .....	9	3.5. Arrangement of the Data .....	13
2.6.d. Secondary Reactions .....	9		

3.5.a. Excited States .....	13
3.5.b. Quenchers .....	13
3.5.c. Data Pages .....	13
3.5.d. Rate Constants .....	13
3.5.e. Comments .....	14
3.6. Experimental Methods .....	14
3.6.a. Excitation Sources .....	14
3.6.b. Analytical Measurements .....	14
3.6.c. Signal Recording .....	14
4. Recent Review Articles .....	14
5. Acknowledgements .....	15
6. Tables of Quenching Data	
1. Aluminum complexes	
2. Cadmium complexes	
3. Cerium complexes	
4. Chromium complexes	
5. Copper complexes	
6. Dysprosium complexes	
7. Europium complexes	
8. Indium complexes	
9. Iridium complexes	
10. Iron complexes	
11. Magnesium complexes	
12. Molybdenum complexes	
13. Neodymium complexes	
14. Osmium complexes	
15. Palladium complexes	
16. Platinum complexes	
17. Rhenium complexes	
18. Rhodium complexes	
19. Ruthenium complexes (except Ru(bpy) <sub>3</sub> <sup>2+</sup> )	
20. Ru(bpy) <sub>3</sub> <sup>2+</sup> by inorganic quenchers	
21. Ru(bpy) <sub>3</sub> <sup>2+</sup> by organic complexes (except MV <sup>2+</sup> )	
22. Ru(bpy) <sub>3</sub> <sup>2+</sup> by MV <sup>2+</sup>	
23. Samarium complexes	
24. Terbium complexes	
25. Tin complexes	
26. Titanium complexes	
27. Tungsten complexes	
28. Uranium complexes	
29. Zinc complexes	
7. Notes on the Tables .....	16
7.1. References to Notes on the Tables .....	28
8. Lists of Abbreviations and Symbols .....	30

## 1. Introduction

Over the past thirty years, the photochemistry and photophysics of metal coordination complexes has been an active area of research, drawing upon and merging with the extensive experience of coordination chemists, spectroscopists, and organic photochemists with regard to the synthesis of compounds, the development of experimental techniques, and an understanding of the kinetics and theories of excited states. The development during this time of fast kinetics techniques (conventional and pulsed-laser flash photolysis, time-resolved spectrofluorimetry) and the use of computers for experimental control and data management has caused this research area to evolve into a mature discipline.

Two very important events occurred almost simultaneously a little more than fifteen years ago that triggered a surge of activity in the field: the recognition of the ability of the luminescent excited state of tris(2,2'-bipyridine)ruthenium(2+) ion ( $\text{Ru}(\text{bpy})_3^{2+}$ ) to photosensitize electron transfer reactions, and the first world-wide energy crisis brought on by the oil embargo as a result of the Yom Kippur War in the Middle East. It was recognized almost immediately that the electron-transfer reactions of the excited state of  $\text{Ru}(\text{bpy})_3^{2+}$  and, by extension, those of other coordination complexes, in fluid solution leads to the formation of energy-rich species which, through the manipulation of their subsequent reactions, can result in the generation of storable fuels. The development of schemes for the photochemical conversion and storage of solar energy involving coordination complexes began in earnest, and with it detailed studies of all the quenching reactions of excited states (electron transfer, energy transfer, proton transfer, etc.) and the chemistry of the products of those processes.

Theoretical treatments soon made the connection between the rate constant of the quenching reaction ( $k_q$ ) and the energetics of the reactants. Existing  $k_q$  data were applied to theory, resulting in a demand for more data to test the theory. As a result, values of  $k_q$  for the reactions of the excited states of many coordination complexes with many quenchers under widely diverse experimental conditions have been published in the literature to date. Up to now, it has been very difficult for researchers to find the values of  $k_q$  they want, or to know exactly what has been done and what has not. In addition, those values of  $k_q$  that have been published in the review literature have not been subjected to a critical evaluation of their quality, nor have they been part of a compilation in which the experimental conditions of their determination, and thus their validity, have been described.

This compilation is devoted to the presentation and critical evaluation of  $k_q$  for dynamic, collisional processes between \*S and Q in fluid homogeneous solution. The excited states have been limited to those of ions and complexes of the inner- and outer-transition metals, and porphyrin complexes of nontransition metals. Quenchers include inorganic and organic species, as well as the ground state of the substrates. In addition to displaying the  $k_q$  values for excited state/quencher couples and the literature reference for the source of the rate constant, the tables contain descriptions of the solution medium, the temperature at which the experiment was performed, the experimental method used, the range of [Q] used, and activation parameters, as well as other pieces of information extracted from the original publications that could be useful to the reader for the evaluation of the quality of the results.

This introduction to the compilation continues, in Sec. 2, with a discussion of the conceptual background to quenching: the excitation of coordination complexes, the decay of the excited states, the types of quenching processes, and the fundamental "Stern-Volmer" kinetics of quenching. Consideration is given to the conditions that lead to deviations from Stern-Volmer behavior, the relationship of the kinetics of diffusion to  $k_q$ , and the efficiency of escape of redox products from the solvent cage as a result of electron-transfer quenching. The structure of the Tables is examined in Sec. 3: the scope of the compilation, the procedures for the selection of values of  $k_q$  from the literature, the problems of nomenclature and speciation, and our concern with the errors and uncertainties that accompany the numerical quantities. The experimental methods used by authors to obtain the data are also described. We offer, in Sec. 4, a list of recent review articles about aspects of the quenching of excited states of coordination complexes that may be useful to the reader. A list of abbreviations and symbols, and the molecular structures of some of the more complicated polymeric and heterocyclic quenchers precede the Tables; the Tables are followed by Notes which describe the mechanisms and equations that have been used in specifically referenced papers for the extraction of the values of  $k_q$ .

## 2. Conceptual Background

### 2.1. Excitation of Substrates

Absorption of light in the ultraviolet, visible, or near-infrared regions of the spectrum by a coordination complex substrate (S) of the general form M-L, where M is the metal center and L represents the ligands in generic terms, results in the generation of electronically excited states within the period of photon absorption ( $\sim 10^{-16}$  s). The subsequent rapid passage of the system along deactivation routes leads to the eventual formation, generally, of the lowest excited state of the substrate (\*S), which is relatively long lived due to the spin restrictions governing its conversion back to the ground state; the efficiency of





Processes II, III, V, and VI can be experimentally demonstrated by the identification of their products as stable compounds or transient intermediates following flash excitation. The experimental evidence for the formation of an exciplex is generally the observation of its absorption or emission in flash photolysis. Energy transfer is experimentally demonstrated if the emission or photoreaction of \*Q is observed. In addition, thermodynamic considerations and comparisons with analogous systems are widely used to suggest the most probable mechanism, at least among energy and electron transfer.

Nevertheless, it remains a challenge to obtain a clear answer concerning the exact nature of the intermediates, inasmuch as the same final products could arise from different "successor complexes" existing simultaneously in the same reaction. Similarly, analogous final products from analogous systems may arise from different successor complexes.

Experimental evidence in favor of a particular quenching process does not exclude the possibility that some fraction of the quenching acts occurs via a different mechanism. The experimentally determined value of  $k_q$  is, however, an overall rate constant representing the sum of the  $k_q$  values for the individual processes; the relative importance of the various processes can only be evaluated indirectly.

## 2.5. Fundamental Quenching Kinetics

The experimental determination of  $k_q$  is based on the measurement of a property ( $\Lambda$ ) that is proportional to the concentration of one or more of the species involved in the overall photochemical process. The mathematical relationship between  $\Lambda$  and  $k_q$  is derived from the assumed mechanism by the use of the usual treatment of time-independent (steady-state) and -dependent kinetics. The derived relationship contains  $\Lambda$  and  $[Q]$  as variables, and  $k_q$  and/or other rate constants as invariant parameters when Q and the other species are present as unique species; the problem of the variation in the nature of Q as a function of solution medium is addressed in Sec. 2.6.b below.

It is obvious that the reliability of the values of  $k_q$  reported by a researcher depends ultimately on the validity of the relationship derived from the assumed mechanism. Evidence in favor of a specific mechanism is generally obtained by the measurement of  $\Lambda$  for a set of experiments in which  $[S]$  is maintained constant and  $[Q]$  is changed across an appropriately wide range (at least one order of magnitude); clearly, the observed dependence of  $\Lambda$  on  $[Q]$  must be that expected for the assumed mechanism. Of course, a mechanism may be assumed, and  $k_q$  evaluated at only one  $[Q]$ ; such a procedure, however, does not give any evidence for the mechanism, and the quality of the value of  $k_q$  determined in that way is open to question. It is important to note that the values of  $k_q$  are always related to  $k_{de}$ , which is the sum of the rate constants of all the deactivation processes of \*S-Q. The relative contribution of each deactivation mode to the over-all quenching process can be evaluated, in principle, through additional measurements; this point, however, will not be discussed further.

The most commonly measured properties ( $\Lambda$ ) are the intensity of emission from \*S under continuous steady-state excitation, and the decay of emission from \*S, or absorption by \*S, after pulsed excitation.

By assuming that the quenching mechanism is represented by reactions (1)-(5), application of the the steady-state treatment, where  $d[*S]/dt = 0$  and  $[S]_{ss}$  is the steady-state concentration of \*S [Eq. (17)], leads to the relationship [Eq. (18)] between  $k_q$  and the intensity of the emission from \*S in the absence ( $I_l^0$ ) and presence ( $I_l$ ) of Q.

$$[*S]_{ss} = \frac{I_a \eta^*}{k_0 + k_q [Q]}, \quad (17)$$

$$I_l^0 / I_l = 1 + (k_q / k_0) [Q]. \quad (18)$$

Similarly, by defining the lifetime of \*S in the presence of Q as  $\tau = 1/(k_0 + k_q [Q])$ , an equivalent relationship [Eq. (19)] between the lifetime of \*S can also be derived from the expressions describing the time-dependent behavior of the concentrations of the species.

$$\frac{\tau_0}{\tau} = 1 + (k_q / k_0) [Q] \quad (19)$$

These are the Stern-Volmer (S-V) relationships that are very widely used in the evaluation of  $k_q$ . The S-V constant ( $K_{SV}$ ) is defined as

$$K_{SV} = k_q / k_0 = k_q \tau_0 \quad (20)$$

S-V plots of  $I_l^0 / I_l$  vs  $[Q]$  or  $\tau_0 / \tau$  vs  $[Q]$  are predicted, by Eqs. (18) and (19), to be linear with slopes equal to  $K_{SV}$ , provided that Q does not absorb the exciting and emitting light, or that appropriate corrections have been made.

Similarly, if reaction (4) leads to a product, the quantum yield of which can be measured in the absence ( $\Phi_0$ ) and presence ( $\Phi$ ) of Q, Eq. (21) predicts that a plot of  $\Phi_0/\Phi$  vs [Q] be linear:

$$\Phi_0/\Phi = 1 + K_{SV}[Q] \quad (21)$$

If reaction (5) leads to a product, the quantum yield of which is determined as a function of [Q], the steady-state treatment of the quenching mechanism predicts that a plot of  $1/\Phi$  vs [Q] be linear with an intercept/slope ratio equal to  $K_{SV}$ .

The calculation of  $k_q$  from  $K_{SV}$ , requires the independent measurement of  $\tau_0$  under the same experimental conditions in order for a value of  $k_q$  to be obtained. The use of a value of  $\tau_0$  measured under different conditions implies that  $\tau_0$  is independent of the change in the conditions, an assumption that must be proven for the value of  $k_q$  to be valid.

If the quenching is assumed to involve reaction (6) instead of (5), a contribution from \*S-Q to the emission intensity under continuous excitation should, in principle, be taken into consideration, which results in Eqs. (22)-(24), where  $\gamma = \beta'k_{rd}'/\beta k_{rd}$ , and  $\beta$  and  $\beta'$  are the ratios of the intensity of the emission at the selected wavelength and that under the entire emission band for \*S and \*S-Q, respectively.

$$[*S]_{ss} = \frac{I_a \eta^* (k_{-d} + k_{de})}{k_0(k_{-d} + k_{de}) + k_{de}k_d[Q]}, \quad (22)$$

$$[*S-Q]_{ss} = \frac{I_a \eta^* k_d[Q]}{k_0(k_{-d} + k_{de}) + k_{de}k_d[Q]}, \quad (23)$$

$$\frac{I_l^0}{I_l} = \frac{\left[ 1 + \frac{k_d k_{de}[Q]}{k_0(k_{-d} + k_{de})} \right]}{1 + \gamma \left[ \frac{k_d[Q]}{k_{-d} + k_{de}} \right]}. \quad (24)$$

Clearly, a plot of  $I_l^0/I_l$  vs [Q], based on Eq. (24), is not linear; the plot has a negative deviation from linearity, and reaches a plateau for  $[Q] \rightarrow \infty$ . The limiting value of  $I_l^0/I_l$  for  $[Q] \rightarrow \infty$  is  $k_{de}/\gamma k_0$ , with  $k_{de} > \gamma k_0$ . When  $\gamma = 0$ , i.e. when no emission occurs from \*S-Q, Eq. (24) reduces to Eq. (25), which is identical to Eq. (18) via Eq. (7).

$$\frac{I_l^0}{I_l} = 1 + \left[ \frac{k_d k_{de}}{k_0(k_{-d} + k_{de})} \right] [Q] \quad (25)$$

Even if  $\gamma \neq 0$ , the nonlinearity predicted by Eq. (24) is commonly not perceived because of the limitations of the experiment. The initial portion of the plot of  $I_l^0/I_l$  vs [Q] can be observed to be linear within the experimental error when  $k_d[Q] < (k_{de} + k_{-d})$ , i.e.,  $[*S-Q]_{ss} < [*S]_{ss}$ . However, the initial slope has a value of  $k_d(k_{de} - \gamma k_0)/[k_0(k_{-d} + k_{de})]$  which is not equal to  $k_q/k_0$  via Eq. (7). Only if  $k_{de} \gg k_0$ , which is the usual case, will the initial slope approximate  $K_{SV}$ .

The steady-state approximation cannot be applied to the concentrations of intermediates following the absorption of light from a short-lived source. The solution of differential equations (26) and (27), that describes the dependence of the concentrations of \*S and \*S-Q as a function of time  $t$ , results in Eqs. (28) and (29), assuming that  $[*S] = [*S]_0$  and  $[*S-Q] = 0$  at  $t = 0$ .

$$\frac{d[*S]}{dt} = k_{-d} [*S-Q] - (k_{rd} + k_{nr} + k_{rx} + k_d[Q]) [*S], \quad (26)$$

$$\frac{d[*S-Q]}{dt} = k_d [*S][Q] - (k_{-d} + k_{de}) [*S-Q], \quad (27)$$

$$[*S]_t = C_1 [*S]_0 \exp(-m_1 t) + C_2 [*S]_0 \exp(-m_2 t), \quad (28)$$

$$[*S-Q]_t = C_3 [*S]_0 [\exp(-m_2 t) - \exp(-m_1 t)], \quad (29)$$

where

$$\begin{aligned} m_1 &= \frac{1}{2}(k_0 + k_{de} + k_{-d} + k_d[Q]) + \frac{1}{2}R^{1/2}, \\ m_2 &= \frac{1}{2}(k_0 + k_{de} + k_{-d} + k_d[Q]) - \frac{1}{2}R^{1/2}, \end{aligned} \quad (30)$$

$$R = (k_0 + k_{de} + k_{-d} + k_d[Q])^2 - 4(k_0k_{-d} + k_0k_{de} + k_{de}k_d[Q]),$$

and

$$\begin{aligned} C_1 &= (k_0 + k_d[Q] - m_2)/(m_1 - m_2), \\ C_2 &= (m_1 - k_0 - k_d[Q])/(m_1 - m_2), \\ C_3 &= \frac{(k_0 + k_d[Q] - m_2)(m_1 - k_0 - k_d[Q])}{k_{-d}(m_1 - m_2)}. \end{aligned}$$

According to these equations, [\*S] decreases with time via biexponential kinetics, while [\*S-Q] increases at short times, reaches a maximum, and then decreases. With increasing [Q],  $m_1$  increases monotonically while  $m_2$  reaches a limiting value of  $m_2(\text{lim}) = k_{de}$ . The limiting value of  $m_2$  at [Q] = 0 is  $k_0$ .

In most cases, however, the faster component of the decay of \*S, and the grow-in period of \*S-Q occur in times too short with respect to the resolution time of the apparatus; only the slower component of the decay is experimentally observed, and is identical for both \*S and \*S-Q. Under such conditions, provided that Q is not consumed to any significant extent during the time period of the experiment, the observed decay follows pseudo-first order kinetics; the apparent rate constant,  $m_2$  can be evaluated and a lifetime of \*S under quenching conditions,  $\tau = 1/m_2$ , can be defined. In spite of the apparent differences between Eqs. (24) and (30), the plot of  $m_2/k_0 = \tau_0/\tau$  versus [Q] from Eq. (30) is quite similar to that of  $I_1^0/I_1$  versus [Q] from Eq. (24). As with the intensity plot described above, the experimentally measurable portion of the  $\tau_0/\tau$  plot generally appears to be linear within the experimental error, with an initial slope equal to  $k_d(k_{de} - k_0)/(k_{-d} + k_{de} - k_0)$ , which is approximately equal to  $K_{SV}$  if  $k_{de} \gg k_0$ . Under these conditions, Eq. (31) is valid when  $\tau = 1/m_2$ .

$$\frac{\tau_0}{\tau} = 1 + \left[ \frac{k_d k_{de}}{k_0(k_{de} + k_{-d})} \right] [Q] = 1 + (k_q/k_0) [Q] = 1 + K_{SV}[Q] \quad (31)$$

It is clear that whenever the approximations mentioned above are valid, the quenching of emission intensity and the quenching of the excited-state lifetime are exactly coincident. The lack of such coincidence is generally taken as evidence for a more complex mechanism, although this may not necessarily be the case.

## 2.6. Other Considerations of the Kinetics

There are several factors that cause the kinetics of quenching to become more complex than expected from the S-V equations.

### 2.6.a. Effect of Ionic Strength

When both S and Q are ionic species, the value of  $k_q$  is a function of the ionic strength of the solution ( $\mu$ ). Because  $\mu$  will change as [Q] is changed, the value of  $k_q$  thus obtained will no longer be a constant for a set of measurements, with the result being that the observed relationship between  $\Lambda$  and [Q] may be different from that expected for the proposed mechanism. In order for  $k_q$  to remain constant for a set of experiments in which [Q] is changed, it is necessary for  $\mu$  to be maintained constant through the addition of appropriate amounts of an inert electrolyte. Due consideration must be given to the possibility that pairing of the presumed innocent added ions with S and/or Q can change the kinetic properties of \*S and its successors.

Often,  $k_q$  is evaluated from measurements at very low [Q] in the absence of added electrolyte, where effects due to variations in the low values of  $\mu$  are probably negligible; such values, obtained in the presence of low [S], can be taken as approximating of  $k_q$  in the limit of  $\mu \rightarrow 0$ . Other methods of obtaining limiting values of  $k_q$  from measurements at constant (but variable)  $\mu$  involve the use of the Debye-Huckel equations (subject to the usual limitations in their use) or, more valuably, the extrapolation of a plot of  $k_q(\mu)$  vs an appropriate semi-empirical function of  $\mu$  (e.g.,  $\mu^{1/2}$ ).

### 2.6.b. Multiple Forms of the Quencher

If, in solution, Q is involved in equilibrium reaction (32) (e.g. acid-base, metal ion complexation, etc.) among its various  $i$  forms ( $Q_a$ ,  $Q_b$ ,  $Q_c$ , etc.), the quenching process can occur from some or all of the Q species, and will be a function of the solution medium parameters that affect the position of equilibrium. For experimental convenience,  $\Lambda$  is generally determined as a function of the total concentration of Q ( $[Q]_{\text{tot}}$ ), where  $[Q]_{\text{tot}} = \sum[Q_i]$ , and the mole fractions of each of the species ( $X_i$ ) is expressed as  $X_i = [Q_i]/[Q]_{\text{tot}}$ .



If the values of  $X_i$  are independent of  $[Q]_{\text{tot}}$ , the value of  $k_q$  can be obtained in the usual way, where  $k_q$  is actually the weighted average of the quenching rate constants for the individual forms:  $k_q = \sum X_i k_q(Q_i)$ . Because  $X_i$  is a function of the solution medium, it is possible, in principle, to obtain the specific values of  $k_q(Q_i)$  through the judicious control of the medium. If, on the other hand,  $X_i$  changes with  $[Q]_{\text{tot}}$ , the concept of an average value of  $k_q$  is meaningless and the constant cannot be calculated. The specific  $k_q(Q_i)$  values can be estimated from measurements in various solution media by means of appropriate algebraic procedures (e.g., best-fitting routines), provided that  $X_i$  can be independently determined for each experimental condition.

#### 2.6.c. Non-selective Measurements

If the analytical methods used in the quenching experiments are not selective, and reflect the concentrations (and their changes) of  $^*S$  and species that originate directly or indirectly from the quenching step (i.e., exciplex), nonlinear S-V plots for emission intensity under steady-state conditions and very complex time-dependent behavior of the system under pulse conditions may be observed. Very severe assumptions are often required to derive appropriate kinetics equations, and to calculate  $k_q$ .

#### 2.6.d. Secondary Reactions

Measurements based on the quantum yields of photochemical products may be affected by secondary thermal and/or photochemical reactions. For example, the primary products of an electron transfer quenching reaction are frequently consumed (and even depleted) through back electron transfer reactions to form the ground state reactants. Secondary reactions must be included into the mechanistic scheme, and the corresponding kinetic equation must be used to calculate  $k_q$ . It is worth noting that data obtained from such systems have a larger uncertainty than those obtained by means of the usual S-V equations; moreover, assumptions about unknown parameters are often required.

#### 2.6.e. Partially Unquenchable Reactions

If a photochemical reaction originates from two excited states of the substrate, but only one state is quenched, Eq. (21) applies only to the quantum yield of the quenchable part of the reaction, while experimentally, the measured quantum yield is the sum of those quantities for both the quenchable and unquenchable parts of the reaction. Appropriate corrections must be made to the experimental values of  $\Phi_0$  and  $\Phi$  in order for  $k_q$  to be calculated.

#### 2.6.f. Quenching of a Higher-Energy Excited State

It is possible that a compound used for quenching  $^*S$  is also capable of quenching a higher-energy excited state of the substrate,  $^{**}S$ , at the same time. If  $^*S$  originates from the intramolecular deactivation of  $^{**}S$ , the quenching of  $^{**}S$  causes the population of  $^*S$  and the resulting luminescence to follow a quadratic dependence on  $[Q]$ . However, the lifetime of  $^*S$  is generally unaffected by the involvement of short-lived  $^{**}S$ .

#### 2.6.g. Static Quenching

If the substrate and quencher form labile adducts in the ground state, such as the case of ion-pairs between ions of different signs, excitation of  $S$  in the adduct results in the quenching of the emission from  $^*S$  due to intramolecular interactions within the adduct; the extent of adduct formation is governed by the concentrations of  $S$  and  $Q$ , and the equilibrium constant of the process. As a result, the population of  $^*S$  and the resulting luminescence and photoproduct formation is less than that occurring in the absence of static quenching, and is a complex function of  $[S]$  and  $[Q]$ . The existence of static quenching does not affect the lifetime of  $^*S$  after pulsed excitation.

### 2.7. Corrections of $k_q$ for Diffusion

When quenching is viewed as occurring via reaction (6),  $k_q$ , as defined by Eq. (7), is approximately equal to  $k_d k_{de}/k_{-d}$  when  $k_{de} \ll k_{-d}$ , and to  $k_d$  when  $k_{de} \gg k_{-d}$ . In the latter case, in order to reveal the relative importance of  $k_{de}$  in a homologous series of quenching processes, it is often convenient to use the classical Noyes theory of diffusional reactions to obtain a rate constant ( $k_{\text{cor}}$ ) for the final step of a reaction, exclusive of diffusion. From the theory, this rate constant is calculated via Eq. (33):

$$1/k_{\text{cor}} = 1/k_q - 1/k_d \quad (33)$$

When the mechanism of quenching is given by reaction (6), the expression for  $k_q$  in Eq. (7) can be substituted into Eq. (33), yielding Eq. (34). which is an expression for  $k_{\text{cor}}$  in terms of the elementary processes in reaction (6).

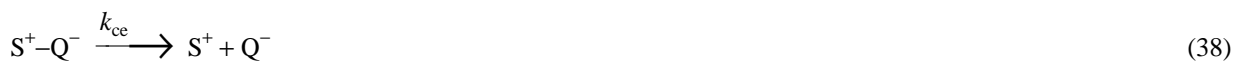
$$k_{\text{cor}} = k_{\text{d}}k_{\text{de}}/k_{-\text{d}} \quad (34)$$

When  $k_{\text{q}} \ll k_{\text{d}}$ ,  $k_{\text{cor}} \sim k_{\text{q}}$ ; when  $k_{\text{q}} \sim k_{\text{d}}$ ,  $k_{\text{cor}} > k_{\text{q}}$ . We have included  $k_{\text{cor}}$  values in this compilation only when the corresponding values of  $k_{\text{q}}$  were not reported in the original publication and could not be easily calculated from  $k_{\text{cor}}$ .

## 2.8. Cage Escape Efficiency

Because of the importance of electron transfer quenching to potential applications of photosensitization, it is important to know the efficiency with which the primary products of electron transfer escape back electron transfer within the solvent cage and diffuse freely into the bulk solution. The major experimental approaches for the determination of this quantity ( $\eta_{\text{ce}}$ ) are the measurement of the quantum yield of formation of a primary product (e.g.,  $\Phi(\text{S}^+)$  for  $\text{S}^+$  from oxidative quenching) under continuous irradiation, and the measurement of  $[\text{*S}]$  and the concentration of one of the primary products of quenching after pulsed excitation; the latter technique requires that the molar absorptivities of the two species be known in order to effect the conversion of absorbance to concentration. When the measurement of  $\Phi(\text{S}^+)$ , for example, is used as the basis of the determination of  $\eta_{\text{ce}}$ , care must be taken to account for the back electron transfer reaction of the redox products of quenching in the bulk solution, or to avoid it completely by the use of a selective sacrificial scavenger for one of the products. These secondary reactions must be included in the overall mechanism from which the kinetic equation for  $\Phi(\text{S}^+)$  is derived.

If the quenching is assumed to occur via reactions (1)-(4), (6), and (35)-(38), a steady-state treatment leads to Eq. (39).



$$\Phi(\text{S}^+) = \eta^* \left[ \frac{k_{\text{q}}[\text{Q}]}{k_{\text{q}}[\text{Q}] + k_0} \right] \left[ \frac{k_{\text{et}}}{k_{\text{et}} + k_{\text{oq}}} \right] \eta_{\text{ce}} \quad (39)$$

where

$$k_{\text{q}} = k_{\text{d}}(k_{\text{bt}} + k_{\text{oq}}) / (k_{\text{bt}} + k_{\text{oq}} + k_{-\text{d}}) \quad (40)$$

and

$$\eta_{\text{ce}} = \frac{k_{\text{ce}}}{k_{\text{ce}} + k_{\text{bt}}} \quad (41)$$

Inasmuch as  $\eta^*$ ,  $k_0$ ,  $k_{\text{q}}$ , and  $\Phi(\text{S}^+)$  can be experimentally determined, the quantity  $f$  can easily be evaluated by the use of its defining Eq. (42).

$$f = \left[ \frac{k_{\text{et}}}{k_{\text{et}} + k_{\text{oq}}} \right] \eta_{\text{ce}} \quad (42)$$

It is important to note that  $f$  represents the fraction of all the quenching acts that eventually leads to the production of electron transfer products in the bulk solution. Only when electron transfer is the sole quenching process ( $k_{\text{oq}} = 0$ ) does  $f$  represent the cage escape efficiency in electron transfer quenching.

## 3. Explanation of the Tables

### 3.1. Scope of the Compilation

The compilation is complete through the end of 1986. The computer search of the bibliographic data base of the Radiation Chemistry Data Center (RCDC) of the University of Notre Dame, using the names of the metals and "porphyrin" as

keywords, the personal literature files of the authors, and an examination of cross-referenced papers yielded a list of publications in books, serials, and periodicals which were then critically examined. Publications of limited diffusion, such as dissertations, theses, and abstracts of conferences, were not included for examination.

### 3.2. Procedures of Selection

In order to be included in this compilation, values of  $k_q$  had to be explicitly given in the published paper, or capable of being calculated by us from values of  $K_{SV}$  and  $\tau_0$  reported in the same paper, or from the values of  $k_0$ ,  $k_d$ ,  $k_{-d}$ , and  $k_{de}$  reported in the paper, and the use of Eq. (7). No values of  $k_q$  were extracted from graphical treatments, nor were any calculated from  $K_{SV}$  and  $\tau_0$  taken from different sources.

The rate constant of quenching is that of a dynamic process occurring in a fluid solution in which there is the uniform distribution of substrate and quencher. Data concerning systems in which either the substrate or the quencher, but not both, might be preferentially confined to localized regions of a microenvironment, such as in the presence of micelles and polyelectrolytes, were accepted only if there was clear evidence that quenching requires the diffusion of at least one species through the medium.

In addition, preference was given to data concerning sufficiently well characterized chemical species obtained under sufficiently well defined experimental conditions. Data concerning poorly defined systems were included in the compilation only if more precise reports were lacking; we have taken the point-of-view that poor data are better than none at all, as long as the reader is provided with the information to evaluate the quality of the result.

We have found, not unexpectedly, the repetition of the same values of  $k_q$  for the same excited state/quencher couple under the same experimental conditions from the same laboratory in a number of references. In this case, reference is made only to the paper containing the largest amount of information and/or published in the most widely disseminated journal. The other references, however, are cited in the bibliography, and indication of their existence is made in the tables as a "comment". Occasionally, we have found *different* values of  $k_q$  for the same excited state/quencher couple under the same experimental conditions from the same laboratory; this situation can occur due to the reevaluation of data over the course of time by the authors, their recognition of the limitations in their experimental procedures, or the existence of inadvertent typographical errors. In this case, we have made a critical evaluation, on the basis of the information available, of the quality of the values, and have chosen one for display; as before, the other references are cited in the bibliography, and the alternative values are indicated as a "comment".

For some very well-studied systems, there are multiple reports from different laboratories for the same excited state/quencher couple under the same, or very similar, experimental conditions. In these cases, all values are presented as independent entries for the following reasons. When the values of  $k_q$  are different, we believe that it is impossible for us to establish which value is more valid short of performing the experiment ourselves; the users of these data are urged to make their own evaluation of the quality of the numbers from the information given in the papers based on their own expertise. When the values are the same, or very similar, we have chosen not to average the values and combine the entries so as to avoid the loss of valuable pieces of information contained in the individual papers. To remove entries, we feel, would deprive the reader of the opportunity to make direct comparisons.

### 3.3. Nomenclature and Speciation

For all the coordination compounds, both substrates and quenchers, in this compilation, names and formulas are written with the symbol of the central metal as the initial portion for reasons of alphabetical ordering. Use of abbreviations for the ligands in the substrates were limited to 2,2'-bipyridine (bpy) and 1,10-phenanthroline (phen) and their derivatives, but were widely used for the quenchers as a space-saving measure; a list of all the abbreviations and symbols used appears below in Sec. 6.

The oxidation states of metallic quenchers, as superscripts in Roman numerals to the symbol of the element, are designated only in those cases where the exact nature of the species in solution is unclear. For labile complexes, which require the presence of both the free metal ion and the ligands in solution, the metal ion/ligand ratio ( $[M]/[L]$ ) in the bulk solution is indicated in the "Solution Medium" column of the Tables; labile complexes of unknown formulation, or those that may actually be a mixture of various species in equilibrium are indicated as M-L with the oxidation number of the metal shown.

Organic quenchers are indicated by their names, but the use of abbreviations is very widespread. Names and abbreviations were chosen in an attempt to achieve a delicate balance among several highly desirable features: succinctness, unambiguity, uniformity, and clarity to even those not fluent in organic nomenclature. Therefore, the names used in the compilation may be different than those that appear in the original publications. For organic quenchers with very complicated

structures and correspondingly complicated formal names, such as polymers and heterocycles, generic abbreviations (OrgQue, PolyVio) are used; their structural formulas are shown below in the Figures (Section 7).

In a few cases, the nomenclature is, regrettably, ambiguous, reflecting analogous ambiguities in the original publications.

For the majority of ionic substrates and quenchers, the counterion has not been shown; it has been indicated as a comment in the tables in those few cases in which there is evidence that its presence affects the photophysical properties of the substrate.

In addition to the substitutional equilibria exhibited by some metal complexes discussed above, a number of substrates and quenchers in this compilation undergo equilibrium reactions (e.g., acid-base, monomer-oligomer) in solution, so that the predominant species is a critical function of the solution composition and the total concentration of the substance. In general, the name used is that indicated in the original publication; no attempt was made to identify the predominant species under the experimental conditions used, although where important, information about the species is presented as a "comment". As a result, the reader will find the names of both the acidic and basic forms, for example, in the Tables and Indexes.

A special case is represented by those transition metal ion quenchers that may be present in the solution as fully solvated and/or partially anated species. We have used the symbol of the simple ion (e.g.,  $\text{Co}^{2+}$ ) to indicate the ensemble of these species, the formula of the fully solvated ion (e.g.,  $\text{Co}(\text{H}_2\text{O})_6^{2+}$ ) for that specific species, and abbreviated notations without the solvent molecules (e.g.,  $\text{CoCl}^+$ ,  $\text{CoCl}_3^-$ ) to indicate partially anated species.

For the majority of the substrates reported in the compilation, only the lowest-energy excited state is quenched, and no indication of its term symbol is required to avoid ambiguity. When quenching is experienced by two lowest-energy excited states of a substrate, each state is identified by its spin multiplicity ([singlet] and [triplet] for the upper and lower state, respectively) or, in the case of  $\text{Tb}^{3+}$ , by the usual spectroscopic notations ( $^5\text{D}_3$ ] and  $^5\text{D}_4$ ] for the upper and lower state, respectively).

### 3.4. Errors and Uncertainties

In many cases, values of  $k_q$  are given with an error range or uncertainty estimation in the original publication; however, the criteria used by authors to evaluate the uncertainty in reported values are rarely disclosed, and range from well-defined statistical treatments (e.g., standard deviation) based on multiple replicate experiments, to empirical estimations based on the author's experience. As a result, it is impossible to express the uncertainty in values of  $k_q$  in a uniform way, and we have preferred not to report any errors at all. Similarly, no errors are given for values of  $\tau_0$ ,  $K_{SV}$ , temperature, or any other experimental value.

In addition, we have found that values of  $k_q$  and  $\tau_0$  are reported in the literature with a wide variation of significant figures which, it is presumed, reflects the quality of the data as evaluated by the author. However, in our opinion, the uncertainty in values of  $k_q$  and  $\tau_0$  obtained from independent measurements is unlikely to be less than approximately 10%, even if the reproducibility of the single experimental result is better. As a result, we have reported all  $k_q$  and  $\tau_0$  values with a maximum of two significant figures, unless they were given to only one significant figure in the original publication, or the reported error involves the first figure. Data having an error larger than 40-50% have been labeled with "~". In cases where upper or lower limiting values are reported in the literature, only one significant figure is used.

The same criteria were used for the presentation of activation parameters and other experimental data with the exception of temperature and solute concentrations; in the latter case, for the sake of succinctness, values are given to one significant figure if the second figure is zero.

Despite the fact that rate constants and excited-state lifetimes are functions of temperature, many publications in the literature omit a reference to a specific temperature, or express it in a nonquantitative manner (e.g., "room temperature", "ambient temperature"). In such cases, no temperature is listed. Otherwise, the temperatures or their ranges are listed as presented by the authors. If the uncertainty in the temperature is greater than 1 °C, the "~" label is used.

### 3.5. Arrangement of the Data

For the purpose of browsing, as in the published data tables, the data are divided into twenty-nine sets which are ordered alphabetically according to the name of the metal of the substrate. In the case of ruthenium, which constitutes a large fraction of the total, the entries are subdivided further to display separately  $\text{Ru}(\text{bpy})_3^{2+}$  and inorganic quenchers,  $\text{Ru}(\text{bpy})_3^{2+}$  and organic quenchers except methylviologen (*N,N'*-dimethyl-4,4'-bipyridinium dication;  $\text{MV}^{2+}$ ),  $\text{Ru}(\text{bpy})_3^{2+}$  and  $\text{MV}^{2+}$ , and all other complexes of ruthenium. Entries in the browsing index are linked to individual data pages by a number similar to the table numbers in the published compilation.

### 3.5.a. Excited States

Within each set, the various excited states with the same metal are ordered alphabetically according to the letters in the formula; some formulas denote the exact molecular composition while others incorporate names or abbreviations of the ligands. Singlet states and triplet states of the same molecule are also separated.

### 3.5.b. Quenchers

For any given excited state, the quenchers are divided into two groups: "inorganic" and "organic". Within each group, they are further ordered alphanumerically.

### 3.5.c. Data Pages

The data pages are headed with the name of the excited state and quencher which is repeated with each reported value for the rate constant along with the conditions of the measurement. For any given page, the order of presentation of the data is alphabetical according to the name, formula, or abbreviation of the solvent. For mixed solvent systems, the more abundant solvent is listed first; their ratio (v/v) is given in parentheses. When the ratio is 1:1 and H<sub>2</sub>O is one of the solvents, it is presented first because of the importance of that substance.

Within any given solvent or solvent mixture, the ordering is by ascending values of the temperature, with the explicit value first and the approximate value second. The lowest level of ordering is given to those systems for which no value of the temperature is entered.

Within any temperature group, the ordering is determined by the absence or presence of additional solutes, and by the degree of detail to which the solution medium is known. Systems that consist of the substrate and the quencher as the only solutes are presented first with the "Solution Medium" column blank; thereafter, pH and ionic strength (in units of mol/L; salt used to control ionic strength in parentheses) conditions are given in ascending order, followed by buffers and other solutes in ascending values of their concentrations. Within this hierarchy of ordering, we have attempted to group data obtained in similar media close together.

When more than one additional solute is used in the experiments, we have adopted a specific protocol for the designation of the components, depending to the degree to which the information is specified in the original paper. For example, if both LiCl and NaCl were present, the designation "LiCl and NaCl" is used. However, if independent measurements were made on solutions containing LiCl and NaCl separately which gave the same value of  $k_q$ , "LiCl, NaCl" is shown. If, on the other hand, experiments were performed with either LiCl or NaCl, but the actual contents are not specified, "LiCl or NaCl" is displayed.

### 3.5.d. Rate Constants

Values of  $k_q$  are given in the units of  $L mol^{-1} s^{-1}$  for the second-order reaction. Values of  $k_{cor}$  are reported here, and are labelled as "(corr)". For values of  $k_q$  calculated by us from  $K_{SV}$  and  $\tau_0$  values, or  $k_0$ ,  $k_d$ ,  $k_{-d}$ , and  $k_{de}$  values appearing in the same paper, the indicator "(calc)" is appended.

### 3.5.e. Comments

The Comments contain a wealth of information in essentially this order: the quenching mechanism (if uncertain, "?" is added); the experimental method used in the evaluation of  $k_q$ ; the lifetime of \*S in the absence of quencher ( $\tau_0$  in the absence of air,  $\tau_{0superair}$  in air-equilibrated solutions,  $\tau_{0superund}$  in solutions of unknown O<sub>2</sub> content); the experimental method used for the determination of the lifetime in the absence of quencher, or the literature reference for the value used; the range of [Q] used over which the value of  $k_q$  was determined, and, presumably, is valid; activation parameters; acid-base properties of \*S; references to duplicate or alternative entries; other relevant information. Values of  $f$ , the fraction of the quenching acts that yield electron-transfer products in the bulk solution, are reported here; when  $\eta^* < 1$ , the value of  $\eta^*$  used in its calculation is also given. References in the "Comments", are presented as the RCDC bibliographic number as a link to the full citation.

## 3.6. Experimental Methods

The methods used to obtain  $k_q$  are listed in the comments as follows: excitation source/analytical measurement/signal recording. The same listing appears in parentheses after the value of, say,  $\tau_0$  if the latter quantity was independently determined in the paper. If the method used for  $k_0$  and, say,  $\tau_0$  is the same, no additional listing is given. If the lifetime was taken from the literature, the RCDC number of the reference is given in parentheses.

If more than one experimental method was used, and both methods gave the same value of  $k_q$ , both are listed. When we do not know which one of the two methods was actually used to obtain the reported  $k_q$  value they are joined by the word or.

### 3.6.a. Excitation Sources

The excitation of the substrate is accomplished by means of two main types of light sources: steady-state lamps and lasers that provide a continuous light beam that is monochromatic or that can be passed through a wavelength selection device; pulsed lamps, lasers, or spark gaps that emit a flash of light with a short duration (ns to  $\mu$ s). The intensity of steady-state sources can also be modulated.

### 3.6.b. Analytical Measurements

Values of  $k_q$  are calculated on the basis of one or more of the following analytical measurements:

- (i) intensity of the luminescence of \*S, either as an instantaneous measurement during continuous excitation or as a function of time after pulsed excitation, with the intensity being proportional to [\*S];
- (ii) absorbance of \*S, measured as a function of time after pulsed excitation, with the magnitude of the absorbance being proportional to [\*S];
- (iii) amount of a photoproduct produced during a period of continuous or pulsed excitation, which, from the independent knowledge of the intensity of the monochromatic light absorbed by the substrate, can be converted into the quantum yield of formation of the product;
- (iv) intensity of luminescence from \*Q as an instantaneous measurement during continuous excitation;
- (v) photocurrent and electric conductivity, which are generally measured as a function of time after pulsed excitation.

### 3.6.3. Signal Recording

Luminescence intensity, absorbance, photocurrent, and conductivity methods result in the generation of an electric signal that can be recorded as a function of the time elapsed after pulsed excitation. Each signal can be recorded independently as a single shot, or many signals from the same system may be collected together and averaged, generally via computer, in order to increase the signal/noise ratio and improve the quality of the value of  $k_q$  that results.

## 4. Recent Review Articles

- "Quenching and sensitization processes of coordination compounds." Balzani, V.; Moggi, L.; Manfrin, M.F.; Bolletta, F.; Laurence, G.S., *Coord. Chem. Rev.* **15**: 321-433 (1975) [757372]
- "Investigation of the formation of complexes of organic molecules and lanthanide ions in solutions by the electronic energy transfer method." Ermolaev, V.L.; Sveshnikova, E.V.; Shakhverdov, T.A., *Russ. Chem. Rev.* **45**: 896-912 (1976) Translated from: *Usp. Khim.* **45**: 1753-81 (1976) [766648]
- "Redox properties of polymetallic systems." Meyer, T.J., *Adv. Chem. Ser.* **150**: 73-84 (1976) [76Z027]
- "The use of quenching and sensitization techniques for the study of excited-state properties of transition metal complexes." Balzani, V.; Moggi, L.; Bolletta, F.; Manfrin, M.F., *Adv. Chem. Ser.* **150**: 160-171 (1976) [76Z028]
- "Electronic energy transfer processes involving coordination compounds." Natarajan, P., *J. Sci. Ind. Res.* **36**: 256-67 (1977) [77Z090]
- "Optical and thermal electron transfer in metal complexes." Meyer, T.J., *Acc. Chem. Res.* **11**: 94-100 (1978) [78Z005]
- "The photonics of porphyrin molecules." Dilung, I.I.; Kapinus, E.I., *Russ. Chem. Rev.* **47**: 43-53 (1978) Translated from: *Usp. Khim.* **47**: 83-100 (1978) [78Z075]
- "Photochemistry of porphyrins and their metal complexes in solution and organized media." Whitten, D.G., *Rev. Chem. Intermed.* **2**: 107-38 (1978) [78Z146]
- "Bimolecular electron transfer reactions of the excited states of transition metal complexes." Balzani, V.; Bolletta, F.; Gandolfi, M.T.; Maestri, M., *Top. Curr. Chem.* **75**: 1-64 (1978) [78Z170]
- "Electron transfer photoreactions of porphyrins." Mauzerall, D., *Porphyrins*, D. Dolphin (ed.), N.Y., Academic, 1978, Vol. 5, Part C, p. 29-52 [78Z217]
- "Light-induced electron transfer reactions in solution, organized assemblies and at interfaces: scope and potential applications." Whitten, D.G.; DeLaive, P.J.; Foreman, T.K.; Mercer-Smith, J.A.; Schmehl, R.H.; Giannotti, C., *Solar Energy, Chemical Conversion and Storage*, R.R. Hautala, R.B. King and C. Kotal (eds.), Humana Press Inc., Clifton, NJ, Pub. 1979, p. 117-40 [78Z256]
- "Nonradiating energy transfer and  $\tau$ -metry in use for studying the complexing of rare earth element ions." Antipenko, B.M.; Privalova, T.A., *Koord. Khim.* **4**: 1149-69 (1978) [78Z280]
- "Scope and applications of light-induced electron-transfer reactions of metal complexes for energy conversion and storage." DeLaive, P.J.; Whitten, D.G.; Giannotti, C., *Adv. Chem. Ser.* **173**: 236-51 (1979) [79F345]
- "Excited state electron-transfer reactions of transition metal complexes." Balzani, V.; Bolletta, F.; Scandola, F.; Ballardini, R., *Pure Appl. Chem.* **51**: 299-311 (1979) [79Z028]
- "Light-induced electron transfer reactions." Sutin, N., *J. Photochem.* **10**: 19-40 (1979) [79Z056]
- "Photochemical electron transfer reactions in homogeneous solutions." Balzani, V.; Scandola, F., *Photochemical Conversion and Storage of Solar Energy*, J.S. Connolly (ed.), Academic Press, New York, NY, 1981, p. 97-129 [80S076]
- "Photochemical  $H_2$  and  $O_2$  production by water photolysis." Lehn, J.-M., *Photochemical Conversion and Storage of Solar Energy*, J.S. Connolly (ed.),

- Academic Press, New York, NY, 1981, p. 161-200 [80S102]
- "Photoinduced electron-transfer reactions of metal complexes in solution." Whitten, D.G., *Acc. Chem. Res.* **13**: 83-90 (1980) [80Z009]
- "Light induced electron transfer reactions of metal complexes." Sutin, N.; Creutz, C., *Pure Appl. Chem.* **52**: 2717-38 (1980) [80Z352]
- "Metal phthalocyanines and porphyrins as photosensitizers for reduction of water to hydrogen." Darwent, J.R.; Douglas, P.; Harriman, A.; Porter, G.; Richoux, M.-C., *Coord. Chem. Rev.* **44**: 83-126 (1982) [82Z053]
- "Light-induced and thermal electron-transfer reactions." Balzani, V.; Scandola, F., *Energy Resour. Photochem. Catal.*, M. Graetzel (ed.), Academic, New York, NY, 1983, p. 1-48 [83S265]
- "Excited-state electron transfer." Meyer, T.J., *ACS Symp. Ser.* **211**: 157-76 (1983) [83Z032]
- "Electron-transfer reactions in excited states." Sutin, N.; Creutz, C., *J. Chem. Educ.* **60**: 809-14 (1983) [83Z102]
- "Energy-transfer processes of excited states of coordination compounds." Scandola, F.; Balzani, V., *J. Chem. Educ.* **60**: 814-23 (1983) [83Z103]
- "Structural and photochemical probes of electron transfer reactivity." Endicott, J.F.; Kumar, K.; Ramasami, T.; Rotzinger, F.P., *Prog. Inorg. Chem.* **30**: 141-87 (1983) [83Z215]
- "Excited-state electron transfer." Meyer, T.J., *Progress in Inorganic Chemistry*, S.J. Lippard (ed.), Wiley, New York, NY, 1983, Vol. 30, p. 389-440 [83Z232]
- "Photoredox processes in coordination compounds." Natarajan, P., *Proc.-Indian Acad. Sci., Chem. Sci.* **93**: 1003-14 (1984) [84Z391]
- "Exciplex quenching of photo-excited copper complexes." McMillin, D.R.; Kirchoff, J.R.; Goodwin, K.V., *Coord. Chem. Rev.* **64**: 83-92 (1985) [85E277]
- "Dipole-forbidden energy transfer process in solution." Endicott, J.F., *Coord. Chem. Rev.* **64**: 293-310 (1985) [85Z047]

## 5. Acknowledgments

Financial support for the creation of this compilation was provided by a grant from the National Bureau of Standards, Office of Standard Reference Data, to Boston University, and by the Ministero della Pubblica Istruzione (Italy). The Radiation Chemistry Data Center is supported jointly by the National Bureau of Standards, Office of Standard Reference Data and by the Office of Basic Energy Sciences of the Department of Energy. This is Radiation Laboratory Document No. NDRL-3082.

The authors thank Prof. G. Varani (University of Ferrara) for the translation of Russian articles, and Dr. M. D'Angelantonio (FRAE-CNR Institute, Bologna) and Mr. V. Cacciari (University of Bologna) for technical assistance. F.B. and L.M. specifically thank the FRAE-CNR Institute (Bologna) for access to the international computer network.

## 7. Notes on the Tables

In some of the cases reported in this compilation, deviations from the behavior predicted by the simplest mechanism and the approximations of Sec. 2.5 of the Introduction, such as nonlinear Stern-Volmer (S-V) plots and biexponential decays, are experimentally observed, necessitating the use of alternative equations, or the introduction of additional steps to the mechanism in order for values of  $k_q$  to be extracted. In other cases, conditions specific to the chemistry of the species involved have led the authors of the papers to invoke mechanisms that have unusual features. In still others, novel experimental approaches have been employed, requiring the development of new relationships between  $\Lambda$  and the concentration of the species.

In the discussions that follow, the details of these other equations and mechanisms are presented in sufficient detail in order to enable the reader to appreciate the basis for the values of  $k_q$  in those cases. The specific treatments are preceded by the number of the mechanism (e.g., Mech. [1]) which appears in the Comments column of the tables. Within a particular treatment, there are references to specific papers in which variations on the general theme appear.

For the general treatment of the kinetics of quenching, and the definitions of most of the symbols used here, see Sec. 2 of the Introduction.

### Mech. [1] *Nonlinear Stern-Volmer plots*

If the experimental plots of  $I_l^0/I_l$  or  $m_2$  vs  $[Q]$  show a negative deviation from linearity, the approximate Eqs. (25) or (31) of Sec. 2.5 can no longer be applied; rather the general Eqs. (1) or (2) (Eqs. (24) and (30) of Sec. 2.5) should be used.

$$\frac{I_l^0}{I_l} = \frac{\left[ 1 + \frac{k_d k_{de} [Q]}{k_0 (k_{-d} + k_{de})} \right]}{1 + \gamma \left[ \frac{k_d [Q]}{k_{-d} + k_{de}} \right]} \quad (1)$$

$$m_2 = \frac{1}{2}(k_0 + k_{de} + k_{-d} + k_d [Q]) - \frac{1}{2}R^{1/2} \quad (2)$$

where

$$R = (k_0 + k_{de} + k_{-d} + k_d [Q])^2 - 4(k_0 k_{-d} + k_0 k_{de} + k_{de} k_d [Q])$$

*Ref. 79E349.* This is the only case presented in which a nonlinear plot of emission intensity is reported. With the assumption that  $k_{-d} \gg k_{de}$ , Eq. (1) reduces to Eq. (3). Values of  $k_0$  and  $k_{de}$  were obtained independently from lifetime measurements at  $[Q] = 0$  and at very high  $[Q]$ , respectively;  $\gamma$  was evaluated through a best-fitting procedure of the experimental data to Eq. (3), and  $k_q$  was calculated by use of the reduced form of equation (7) of Sec. 2.3:  $k_q = k_d k_{de} / k_{-d}$ .

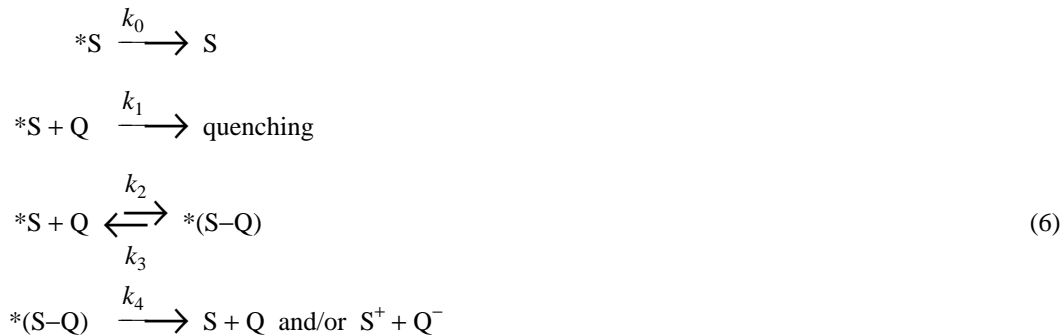
$$\frac{I_l^0}{I_l} = \frac{1 + \left[ \frac{k_d k_{de} [Q]}{k_{-d} k_0} \right]}{1 + \gamma \left[ \frac{k_d [Q]}{k_{-d}} \right]} \quad (3)$$

*Ref. 84E308.* The nonlinear dependence on  $[Q]$  of the rate constant  $k_A$  for the decay of the excited-state absorbance after a flash excitation was interpreted by means of Eq. (4), which is analogous to Eq. (1). Equation (4) was rearranged to Eq. (5). With  $k_0$  known from lifetime measurements at  $[Q] = 0$ ,  $k_q$  was obtained as the intercept/slope ratio of the linear plot of  $k_A$  vs  $(k_A - k_0)/[Q]$ .

$$k_A = k_0 + \frac{\left[ \frac{k_d [Q] (k_{de} - k_0)}{k_{-d} + k_{de}} \right]}{1 + \left[ \frac{k_d [Q]}{k_{-d} + k_{de}} \right]} \quad (4)$$

$$k_A = k_{de} - \left[ \frac{k_{-d} + k_{de}}{k_d} \right] \left[ \frac{k_A - k_0}{[Q]} \right] \quad (5)$$

*Ref. 85A013.* Results analogous to the previous ones were explained by assuming mechanism 6 in which irreversible quenching and the reversible formation of an exciplex are involved.



By assuming that equilibration between \*S and \*(S-Q) exists during the decay ( $k_2[Q]$ ,  $k_3 \gg (k_0 + k_1[Q])$ ,  $k_4$ ) and  $\epsilon(*S) = \epsilon(*(S-Q))$  at the monitoring wavelength, Eq. (7) was obtained, which rearranges to Eq. (8).

$$k_A = \frac{k_0 + \left[ \frac{k_2 k_4}{k_3} + k_1 \right] [Q]}{1 + \left[ \frac{k_2}{k_3} \right] [Q]} \quad (7)$$

$$Y = \frac{k_A - k_0}{[Q]} = \left[ \frac{k_2 k_4}{k_3} \right] + k_1 - \left[ \frac{k_2}{k_3} \right] k_A \quad (8)$$

From decay measurements at various [Q], a linear plot of Y vs  $k_A$  was obtained; values of  $k_2/k_3$  and  $[(k_2 k_4/k_3) + k_1]$  were obtained from the slope and intercept, respectively. The value of  $k_3$  and upper limits for  $k_1$  and  $k_4$  were then calculated by assuming that  $k_2$  is at the diffusion-controlled limit ( $\sim 10^{10} \text{ L mol}^{-1} \text{ s}^{-1}$ ).

The value of the overall quenching constant,  $k_q = k_1 + [k_2 k_4 / (k_3 + k_4)]$ , was calculated by us for this compilation by using the values of the specific rate constants quoted in the original paper.

#### *Mech. [2] Biexponential decay*

*Refs. 82E636 and 83A101.* In these papers, biexponential decays were reported for the quenching of metalloporphyrins and similar complexes. The optical absorbance of the excited state was found to decrease after the flash according to Eq. (9), where  $(\Delta A)_t$  is the difference between the absorbances of the solution at time  $t$  after the flash and before the flash, and  $A_1$  and  $A_2$  are pre-exponential factors.

$$(\Delta A)_t = A_1 \exp(-m_1 t) + A_2 \exp(-m_2 t) \quad (9)$$

A best-fitting procedure was used to evaluate  $m_1$ ,  $m_2$ ,  $A_1$ , and  $A_2$ ; the limiting value of  $m_2$  at high [Q] ( $m_2(\text{lim})$ ) was also obtained. By assuming that the quenching occurs via mechanism 6, the following relationships were written:  $m_1 + m_2 = a + b[Q]$ , where  $a = k_0 + k_3 + k_4$ ,  $b = k_1 + k_2$ , and  $m_2(\text{lim}) = k_4 + [k_1 k_3 / (k_1 + k_2)]$ .

The analysis of numerous pieces of data led the authors to suggest that  $k_1 \ll k_2$  whenever  $m_2(\text{lim}) < k_0$ . Under these conditions, therefore, they assumed that  $k_2 = b$ ,  $k_4 = m_2(\text{lim})$ , and  $k_3 = (a - k_0 - m_2(\text{lim}))$ . The  $k_q$  values presented in this compilation were calculated by us, using Eq. (7) of Sec. 2.3, and the values of  $k_2 (= k_d)$ ,  $k_3 (= k_{-d})$ , and  $k_4 (= k_{de})$  quoted in the original papers.

When  $m_2(\text{lim}) > k_0$ ,  $k_1$  was considered to be no longer negligible with respect to  $k_2$ . This latter rate constant was evaluated (see Kapinus, E.I.; Aleksankina, M.M.; Staryi, V.P.; Boghillo, V.I.; Dilung, I.I. *J. Chem. Soc., Faraday Trans. 2* **81**,

631-42 (1985)) from the pre-exponential factors at various [Q] by means of Eq. (10), assuming  $\epsilon^*(S-Q) = \epsilon^*(S)$ . The values of the other rate constants could then be obtained from  $a$ ,  $b$ , and  $m_2(\text{lim})$ . However, the resulting values of  $k_q$  then become so uncertain that they have not been included in this compilation.

$$\left[ \frac{A_1 m_2 + A_2 m_1}{A_1 + A_2} \right] = k_2 [Q] \left[ \frac{\epsilon^*(S-Q)}{\epsilon^*(S)} \right] + k_3 + k_4 \quad (10)$$

*Mech. [3] Self quenching (ground-state quenching)*

*Ref. 86E677.* In this case Q is S and the emission from \*S must be measured as a function of [S]. Obviously,  $I_a$  is no longer a constant value throughout a set of experiments, but must be evaluated using the Beer-Lambert Law [Eq. (11)], where  $\epsilon$  is the molar absorptivity of S at the excitation wavelength,  $l$  is the optical path length, and  $I_0$  is the intensity of the incident light.

$$I_a = I_0 [1 - \exp(-2.303\epsilon l [S])] \quad (11)$$

By assuming that quenching occurs via reaction (5) of Sect. 2.3, and by introducing Eq. (11) into the steady-state treatment, one obtains Eq. (12), where  $\alpha$  is an instrumental factor.

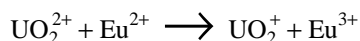
$$\frac{1}{I_l} = \frac{1}{\alpha \beta k_{rd} I_0 \eta^*} \left[ \frac{k_0}{1 - \exp(-2.303\epsilon l [S])} + \frac{k_q [S]}{1 - \exp(-2.303\epsilon l [S])} \right] \quad (12)$$

Equation (12) predicts that a plot of  $1/I_l$  vs [S] will be nonlinear; however, if the absorbance of the solution is  $<0.1$  for all [S] used, Eq. (11) reduces to  $I_a = I_0(2.303\epsilon l [S])$ , leading to Eq. (13), which predicts a linear relationship between  $1/I_l$  and  $1/[S]$  with an intercept/slope ratio of  $k_q/k_0 = K_{SV}$ . The lifetime used to convert  $K_{SV}$  to  $k_q$  must be the limiting value of  $\tau$  as [S]  $\rightarrow 0$ , obtained by extrapolation, for example, from a plot of  $1/\tau$  vs [S]. Note that a linear S-V plot should be obtained from decay measurements for self-quenching, inasmuch as the decay kinetics are not affected by the amount of light absorbed by S.

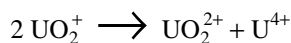
$$\frac{1}{I_l} = \frac{1}{2.303\epsilon l \alpha \beta k_{rd} I_0 \eta^*} \left[ \frac{k_0}{[S]} + k_q \right] \quad (13)$$

*Mech. [4] Quenching by an unstable quencher*

*Ref. 756452.* The quencher ( $\text{UO}_2^{2+}$ ) was produced *in situ* from the substrate ( $\text{UO}_2^{2+}$ ) by means of the following fast reaction:



Addition of  $\text{Eu}^{2+}$  to the solution caused an almost instantaneous decrease of the intensity of  $\text{UO}_2^{2+}$  emission; a slow recovery of the intensity was then observed, which was due to the following disproportionation reaction:



A S-V plot was constructed from the emission intensities measured at various times during the recovery; the corresponding [Q] values were calculated from the initial concentration of  $\text{UO}_2^+$  (equal to the concentration of added  $\text{Eu}^{2+}$ ) and the known rate constant for the disproportionation reaction.  $K_{SV}$  was evaluated from the slope of this linear plot.

*Mech. [5] Quenching of the photoreaction of \*S*

If \*S and \*S-Q undergo photoreaction to product P, the quantum yield for the formation of P after an appropriate period of continuous irradiation,  $t$ , is given by Eq. (14).

$$\Phi(P) = \frac{\int_0^t (k_{rx} [^*S]_{ss} + k_{rx}' [^*S-Q]_{ss}) dt}{\int_0^t I_a dt} \quad (14)$$

If both S and Q are not appreciably consumed during the irradiation period, [\*S]<sub>ss</sub>, [\*S-Q]<sub>ss</sub>, and I<sub>a</sub> can be considered to be constant. Equation (14) can be integrated to Eq. (15).

$$\Phi(P) = \frac{k_{rx}\eta^*(k_{-d} + k_{de}) + k_{rx}'\eta^*k_d[Q]}{k_0(k_{-d} + k_{de}) + k_{de}k_d[Q]} \quad (15)$$

The ratio between the quantum yields in the absence and presence of Q is represented by Eq. (16), where  $\Phi^0(P)$  is the quantum yield at [Q] = 0, and  $\delta = k_{rx}'/k_{rx}$ .

$$\frac{\Phi^0(P)}{\Phi(P)} = \frac{1 + \left[ \frac{k_{de}k_d[Q]}{k_0(k_{-d} + k_{de})} \right]}{1 + \delta \left[ \frac{k_d[Q]}{k_{-d} + k_{de}} \right]} \quad (16)$$

By neglecting the contribution of \*S-Q to the reaction, Eq. (16) is reduced to the S-V Eq. (17) for a quenched photoreaction, which is the same as Eq. (21) of Sec. 2.5.

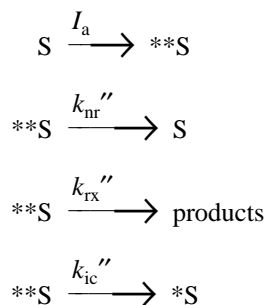
$$\Phi_0/\Phi = 1 + (k_q/k_0)[Q] = 1 + K_{SV}[Q] \quad (17)$$

*Refs. 80F228 and 82E073.* Through the use of Eq. (17),  $k_q$  was evaluated from the slope of a plot of  $\Phi^0(P)/\Phi(P)$  vs [Q].

*Ref. 81E458.* Because Q is S,  $\Phi^0(P)$  could not be measured; Eq. (18), which again neglects the contribution of \*S-Q to the reaction, was used instead of Eq. (17). The slope/intercept ratio of the linear plot of  $1/\Phi(P)$  vs [Q] yields  $K_{SV}$ .

$$1/\Phi(P) = (k_0/k_{rx}) + (k_q/k_{rx})[Q] \quad (18)$$

*Ref. 84A141.* A more complex treatment is required when the measured photoreaction is assumed to originate from both the quenched excited state and a higher-energy, unquenchable excited state, \*\*S, which is directly populated by irradiation. The light absorption step 1 of Sec. 2.2 is substituted by the following steps:



A steady-state treatment leads to Eq. (19). However, a plot of  $\Phi^0(P)/\Phi(P)$  vs [Q] is no longer linear.

$$\Phi(P) = \frac{k_{rx}''}{k_{nr}'' + k_{rx}'' + k_{ic}''} + \frac{\eta_{ic}k_{rx}}{k_0 + k_q[Q]} \quad (19)$$

where  $\eta_{ic} = k_{ic}''/(k_{nr}'' + k_{rx}'' + k_{ic}'')$ .

At high [Q],  $\Phi(P)$  reaches a lower limit given by Eq. (20), which is the quantum yield for the unquenchable reaction from \*\*S.

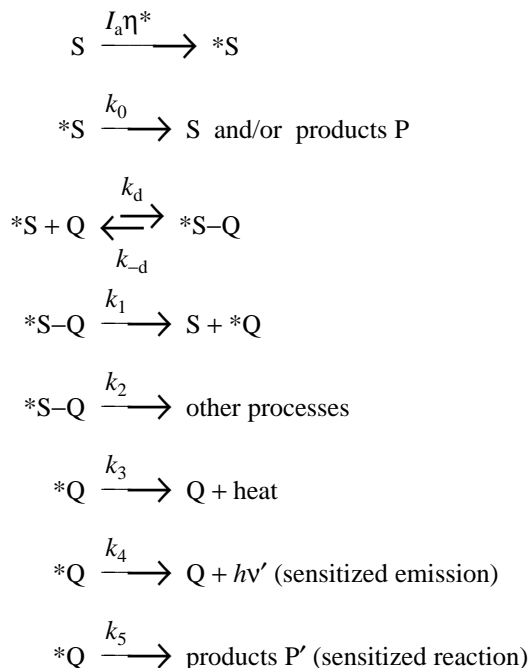
$$\Phi(\text{lim}) = k_{rx}''/(k_{nr}'' + k_{rx}'' + k_{ic}'') \quad (20)$$

If  $\Phi(\text{lim})$  can be evaluated, Eq. (21) can be applied, so that a plot of  $\Phi^0(P)/(\Phi(P) - \Phi(\text{lim}))$  vs [Q] is linear with a slope/intercept ratio equal to  $K_{SV}$ .

$$\frac{\Phi^0(P)}{\Phi(P) - \Phi(\text{lim})} = \left[ \frac{k_0\Phi(\text{lim}) + \eta_{ic}k_{rx}}{\eta_{ic}k_{rx}} \right] + \left[ \frac{(k_0\Phi(\text{lim}) + \eta_{ic}k_{rx})k_q}{k_0\eta_{ic}k_{rx}} \right] [Q] \quad (21)$$

*Mech. [6] Sensitized emission and reaction*

When a quenching process occurs, at least in part, via energy transfer, an excited state of Q, \*Q, is produced which may undergo emission and/or photochemical reaction. The overall quenching constant can then be obtained by measuring the intensity of \*Q emission or the quantum yield of its photoreaction under continuous irradiation. The following mechanism is used to determine  $k_q$ :



The step represented by  $k_1$  has its analogue in the ET step of reactions (12)-(16) in Sec. 2.4;  $k_2$  represents all the other processes involving \*S-Q in reactions (8)-(10) of Sec. 2.3. Thus,  $k_1 + k_2 = k_{de}$ . A steady-state treatment applied to [\*S], [\*S-Q], and [\*Q] leads to Eq. (22) for the emission intensity from \*Q, where  $\alpha$  is an instrumental factor.

$$\frac{1}{I_l} = \left[ \frac{(k_1 + k_2)(k_3 + k_4 + k_5)}{\alpha I_a \eta^* k_1 k_4} \right] + \left[ \frac{k_0(k_{-d} + k_1 + k_2)(k_3 + k_4 + k_5)}{\alpha I_a \eta^* k_1 k_4 k_d} \right] \left[ \frac{1}{[Q]} \right] \quad (22)$$

Provided that Q does not contribute to the absorption of the exciting light, or that an appropriate correction is made, Eq. (22) indicates that a plot of  $1/I_l$  vs  $1/[Q]$  (S-V plot for the sensitized emission) should be linear; indeed, such a linearity is considered as evidence for the mechanism. Under these conditions, the intercept/slope ratio equals  $(k_d(k_1 + k_2))/(k_0(k_{-d} + k_1 + k_2)) = k_q/k_0 = K_{SV}$ .

In an analogous manner, Eq. (23) for the quantum yield of P' production can be written.

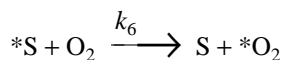
$$\frac{1}{\Phi(P')} = \left[ \frac{(k_1 + k_2)(k_3 + k_4 + k_5)}{\eta^* k_1 k_4} \right] + \left[ \frac{k_0(k_{-d} + k_1 + k_2)(k_3 + k_4 + k_5)}{\eta^* k_1 k_4 k_d} \right] \left[ \frac{1}{[Q]} \right] \quad (23)$$

Equation (23) implies that a linear relationship exists between  $1/\Phi(P')$  and  $1/[Q]$  (S-V plot for the sensitized reaction), provided that Q neither absorbs the exciting light nor is substantially consumed during the irradiation period. From Eq. (23), intercept/slope =  $k_q/k_0 = K_{SV}$ .

*Refs. 80E412 and 86E555.* Emission intensity from the excited quencher was measured under continuous irradiation conditions, and  $k_q$  was calculated by the use of Eq. (22).

*Refs. 85F395 and 86A158.* The quantum yield for the sensitized photoreaction of Q was measured under continuous illumination conditions, and  $K_{SV}$  was evaluated by means of Eq. (23). In the first paper, however,  $k_q$  was evaluated from the

competition between the quenching of \*S by Q and by O<sub>2</sub>, where  $k_6 = 3 \times 10^9 \text{ L mol}^{-1} \text{ s}^{-1}$ .



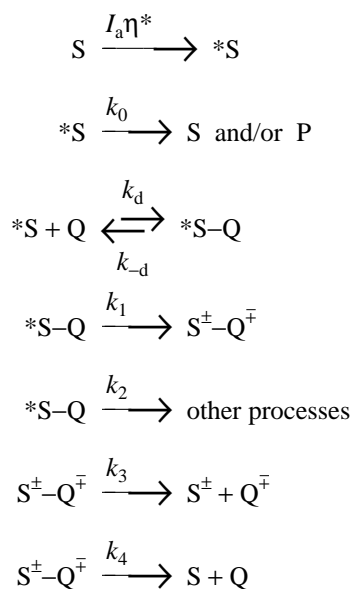
In the presence of O<sub>2</sub>, the steady-state treatment yields Eq. (24).

$$\frac{1}{\Phi(P')} = \left[ \frac{(k_1 + k_2)(k_3 + k_4 + k_5)}{\eta^* k_1 k_5} \right] \left[ 1 + \frac{1}{K_{SV}[Q]} \right] + \left[ \frac{(k_1 + k_2)(k_3 + k_4 + k_5)k_6}{\eta^* k_1 k_5 k_q} \right] \left[ \frac{[O_2]}{[Q]} \right] \quad (24)$$

Equation (24) predicts that a plot of  $1/\Phi(P')$  vs  $[O_2]/[Q]$  will be linear at constant  $[Q]$  with a slope/intercept ratio of  $(k_6/k_q)/(1 + (K_{SV}[Q])^{-1})$ . From  $K_{SV}$  determined in the absence of O<sub>2</sub>,  $k_q$  is obtained.

*Mech. [7] Primary products of electron transfer under continuous irradiation*

If \*S–Q undergoes oxidative transfer (OT) to S<sup>+</sup>–Q<sup>−</sup> or reductive transfer (RT) to S<sup>−</sup>–Q<sup>+</sup>, consideration must be given to the back electron-transfer reactions of the geminate pair (S<sup>±</sup>–Q<sup>∓</sup>) within the solvent cage when evaluation of  $k_q$  is made. The detailed mechanism is as follows:



Application of the steady-state treatment to [\*S], [\*S–Q], and [S<sup>±</sup>–Q<sup>∓</sup>] leads to Eq. (25).

$$[S^\pm-Q^\mp]_{ss} = \frac{I_a \eta^* k_1 k_d [Q]}{\{k_0(k_{-d} + k_1 + k_2) + k_d [Q](k_1 + k_2)\} (k_3 + k_4)} \quad (25)$$

The rate of primary production of S<sup>±</sup> and Q<sup>∓</sup> in the bulk solution is  $d[S^\pm]/dt = d[Q^\mp]/dt = k_3[S^\pm-Q^\mp]$ . The evaluation of  $k_q$  from the quantum yield of S<sup>±</sup> or Q<sup>∓</sup> formation, measured after a finite period of irradiation, is complicated by back electron-transfer reaction (26) between S<sup>±</sup> and Q<sup>∓</sup> in the bulk solution, the rate of which increases with increasing [S<sup>±</sup>] and [Q<sup>∓</sup>]. Different approaches have been used to overcome this difficulty.



*Refs. 78A058 and 80F058.* In these cases, Q<sup>−</sup> is a Co(II) complex which decomposes via a transformation to P' much more rapidly than the occurrence of reaction (26), which can be neglected. Equation (27) results, which predicts a linear

relationship between  $1/\Phi(P')$  and  $1/[Q]$ , with an intercept/slope ratio =  $[k_d(k_1 + k_2)]/[k_0(k_{-d} + k_1 + k_2)] = k_q/k_0 = K_{SV}$ .

$$\frac{1}{\Phi(P')} = \frac{1}{\Phi(Q^-)} = \left[ \frac{(k_1 + k_2)(k_3 + k_4)}{\eta^* k_1 k_3} \right] + \left[ \frac{k_0(k_{-d} + k_1 + k_2)(k_3 + k_4)}{\eta^* k_1 k_3 k_d} \right] \left[ \frac{1}{[Q]} \right] \quad (27)$$

*Ref. 84F351.* In this case, the solution contained a "sacrificial" electron-transfer reagent, X, which was able to react with  $S^-$  to yield S and products with a rate constant  $k_6$ . When [X] is sufficiently high such that reaction (26) is of negligible importance and  $k_6[X] \gg k_5[Q^+]$ , the relationship between  $\Phi(Q^+)$  and [Q] is expressed by Eq. (27).

*Ref. 81A139.* In this case, a similar system was used, but with a concentration of X insufficiently high for reaction (26) to be rendered negligible. Under these conditions, and by assuming that  $k_2 = k_4 = 0$ , Eq. (28) was obtained from a steady-state treatment of  $[*S]$ ,  $[*S-Q]$ ,  $[S^+-Q^-]$ , and  $[S^+]$ .

$$\frac{d[Q^-]}{dt} = I_a \eta^* \left[ \frac{k_q[Q]}{k_0 + k_q[Q]} \right] \left[ \frac{k_6[X]}{k_5[Q^-] + k_6[X]} \right] \quad (28)$$

Equation (28) shows that  $[Q^-]$  does not increase linearly with the irradiation time. The value of  $d[Q^-]/dt$  at a given  $[Q^-]$  was obtained at various [Q] and [X] from the tangent of a plot of  $[Q^-]$  vs irradiation time. The value of  $K_{SV}$  was then obtained as the intercept/slope ratio from the linear plot of  $dt/d[Q^-]$  vs  $1/[Q]$  at constant [X], as expressed by Eq. (29).

$$\frac{dt}{d[Q^-]} = \left[ \frac{k_5[Q^-] + k_6[X]}{I_a \eta^* k_6[X]} \right] + \left[ \frac{k_0(k_5[Q^-] + k_6[X])}{I_a \eta^* k_6[X] k_q} \right] \left[ \frac{1}{[Q]} \right] \quad (29)$$

*Ref. 83A333.* In this case, the same treatment as above was used, but  $d[Q^-]/dt$  was evaluated from the initial slope of the plot of  $[Q^-]$  vs irradiation time.

*Ref. 85F328.* In this case, back electron-transfer reaction (26) was prevented by means of competitive irreversible reaction (30); this latter reaction substitutes for all the reactions of  $S^+-Q^-$  in the previous mechanism.



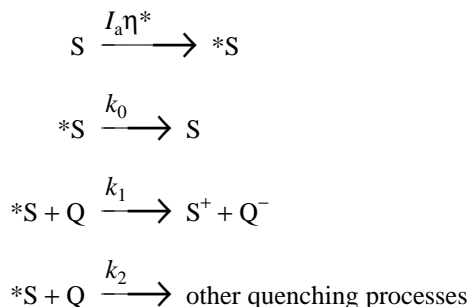
The quantum yield of formation of  $Q^-$  as a function of [Q] is given by Eq. (31).

$$\frac{1}{\Phi(Q^-)} = \left[ \frac{(k_1 + k_2)(k_4 + k_7[X])}{\eta^* k_1 k_7[X]} \right] + \left[ \frac{k_0(k_{-d} + k_1 + k_2)(k_4 + k_7[X])}{\eta^* k_1 k_7[X] k_d} \right] \left[ \frac{1}{[Q]} \right] \quad (31)$$

The plot of  $1/\Phi(Q^-)$  vs  $1/[Q]$  is linear, and the intercept/slope ratio is again equal to  $K_{SV}$ . Note that [X] affects  $\Phi(Q^-)$ , but not  $K_{SV}$ .

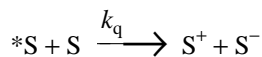
*Mech. [8] Primary products of electron transfer upon pulsed irradiation*

*Ref. 82F065.*  $k_q$  was determined from the measurement of the concentration of a primary product,  $S^+$ , resulting from the flash. The following mechanism was assumed, in which back electron transfer in the bulk solution is neglected:



The quantum yield for the production of  $S^+$  during the flash, assuming that the quenching is irreversible, is  $\Phi(S^+) = k_1[Q]/(k_0 + k_q[Q])$ , where  $k_q = k_1 + k_2$ ;  $1/\Phi(S^+) = (k_q/k_1) + (k_0/k_1[Q])$ . Experimentally,  $\Phi(S^+) = [S^+]_0/I_a \eta^*$ , where  $[S^+]_0$  is the concentration of  $S^+$  just at the end of the flash, evaluated from absorbance measurements at various times after the flash and extrapolated to  $t = 0$  in order to account for back electron transfer. The quantity  $I_a \eta^*$  was obtained from actinometric measurements, using very complex numerical calculations in order to account for the changes in  $[S]$  (and  $[Q]$ , inasmuch as this species absorbs a fraction of the exciting light) during the flash. From the intercept and slope of the linear plot of  $1/\Phi(S^+)$  vs  $1/[Q]$ ,  $k_q$  and the efficiency of formation of the primary products in the bulk solution ( $k_1/k_q$ ) were obtained.

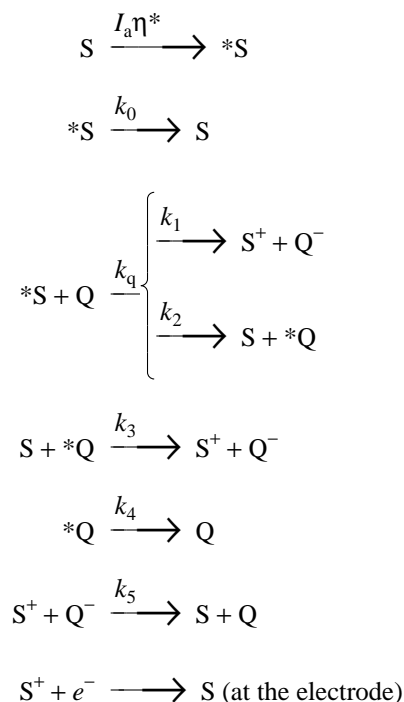
*Ref. 80A023.* The time-dependent variation of the electrical conductivity of the solution after pulsed excitation was used to evaluate  $k_q$  for the following ground-state electron-transfer quenching process:



With the assumption that  ${}^*S-Q$  does not contribute to the reaction, the rate of variation of the conductivity equals the rate of consumption of  ${}^*S$  after the flash as given in Eq. (32).  $k_q$  was obtained from the slope of the linear plot of  $1/t_{1/2}(\text{conductivity})$  vs  $[S]$ .

$$[{}^*S]_t = [{}^*S]_0 \exp\{-(k_0 + k_q[S])t\} \quad (32)$$

*Ref. 80E224.*  $k_q$  was evaluated by means of photocurrent measurements taken after flash excitation. The proposed mechanism is:



Inasmuch as the resolution time of the apparatus was of the order of  $\mu\text{s}$ , the reactions represented by  $k_q$  and  $k_3$  were considered to be complete at  $t = 0$  after the flash. If the reaction represented by  $k_5$  is considered to be of negligible importance during the flash, the concentration of  $S^+$  at  $t = 0$  is given by Eq. (33), where  $I_f$  is the number of photons effectively absorbed by  $1 \text{ dm}^3$  of solution during the flash.

$$[S^+]_0 = \frac{I_f [Q] \{k_1 + (k_2 k_3 [S] / (k_4 + k_3 [S]))\}}{\{k_0 + k_q [Q]\}} \quad (33)$$

By assuming that the reaction at the electrode is diffusion controlled, and by solving the equation describing the diffusion, Eq. (34) is obtained for the intensity of the photocurrent,  $i$ , as a function of time after the flash, from which the product  $\lambda[S^+]_0$ , where  $\lambda$  is a constant, can be evaluated. Inasmuch as  $Q^-$  was initially present in excess before the flash,  $[Q^-]$  is a constant value.

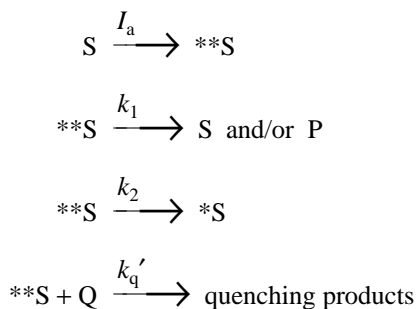
$$i = \lambda[S^+]_0 t^{-1/2} \exp(-k_5 [Q^-] t) \quad (34)$$

A linear plot of  $1/\lambda[S^+]_0$  vs  $1/[Q]$  was obtained experimentally. The rearrangement of Eq. (33) to Eq. (35) shows that the intercept/slope ratio of this plot is equal to  $K_{SV}$ .

$$\begin{aligned}
 \frac{1}{\lambda[S^+]_0} &= \left[ \frac{(k_q / \lambda I_f)}{\{k_1 + (k_2 k_3 [S] / (k_4 + k_3 [S]))\}} \right] + \\
 &\quad \left[ \frac{(k_0 / \lambda I_f)}{\{k_1 + (k_2 k_3 [S] / (k_4 + k_3 [S]))\}} \right] \left[ \frac{1}{[Q]} \right] \quad (35)
 \end{aligned}$$

*Mech. [9] Quenching of higher-energy excited states*

If  $*S$  is indirectly populated from an higher-energy excited state,  $**S$ , and both  $*S$  and  $**S$  are quenched by  $Q$ , the light absorption step 1 of Sec. 2.2 must be substituted by the following reactions:



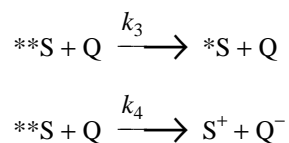
By making the steady-state approximation for [**\*\*S**], [**\*S**], and [**\*S-Q**], and neglecting as usual any emission from **\*S-Q**, one obtains Eq. (36) for the emission intensity of **\*S**, where  $K_{SV}$  is the S-V constant for the quenching of **\*S**, and  $K_h = k_q'/(k_1 + k_2)$ . According to Eq. (36), the S-V plot of  $I_l^0/I_l$  vs [Q] shows a positive deviation from linearity.

$$I_l^0/I_l = 1 + (K_{SV} + K_h)[Q] + (K_{SV}K_h)[Q]^2 \quad (36)$$

On the other hand, in flash experiments the quenching of **\*\*S** results in a decrease of [**\*S**]<sub>0</sub>, but generally has no effect on its decay, provided that the lifetime of **\*\*S** is much shorter than that of **\*S**.

*Ref. 74E519.* Although the S-V plot for  $I_l$  from **\*S** has negative deviation from linearity, its initial slope was taken as equal to  $(K_{SV} + K_h)$  because the quadratic term in Eq. (36) is negligible for [Q]  $\ll$  1 mol/L. In addition,  $K_h$  was considered to be small compared to  $K_{SV}$ ; it is presumed that  $k_q' \sim k_d$ , and  $(k_1 + k_2) \gg k_0$ .

*Ref. 79A220.*  $k_q$  for the quenching of **\*S** was obtained from lifetime measurements in the usual way;  $k_q$  for the quenching of **\*\*S** was determined from the measurement of [**\*S**] and [**S<sup>+</sup>**] at 50  $\mu$ s after the flash. The following quenching modes for **\*\*S** were assumed:



By assuming that at 50  $\mu$ s after the flash all the reactions involving **\*\*S** were completed while those involving **\*S** had proceeded to a negligible extent, Eqs. (37) and (38) were obtained for the concentrations of **\*S** and **S<sup>+</sup>** at that time ( $[\text{*S}]_{50}$  and  $[\text{S}^+]_{50}$ , respectively).

$$[\text{*S}]_{50} = \frac{(k_2 + k_3[Q])I_a}{k_1 + k_2 + (k_3 + k_4)[Q]} \quad (37)$$

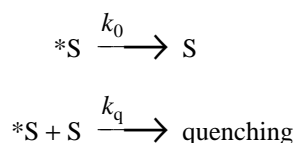
$$[\text{S}^+]_{50} = \frac{k_4[Q]I_a}{k_1 + k_2 + (k_3 + k_4)[Q]} \quad (38)$$

The ratio of Eqs. (37) and (38) yields Eq. (39). From the intercept and slope of the linear plot of  $[\text{*S}]_{50}/[\text{S}^+]_{50}$  vs  $1/[Q]$ ,  $k_2/k_4$  and  $k_3/k_4$  can be evaluated. Values of  $k_3$ ,  $k_4$ , and  $k_q (= k_3 + k_4)$  were obtained by assuming that  $k_2$ , the rate constant for intersystem crossing between **\*\*S** and **\*S**, is in the range  $10^7$ - $10^8$  s<sup>-1</sup>.

$$\frac{[\text{*S}]_{50}}{[\text{S}^+]_{50}} = \left[ \frac{k_3}{k_4} \right] + \left[ \frac{k_2}{k_4} \right] \left[ \frac{1}{[Q]} \right] \quad (39)$$

#### *Mech. [10] Quenching in the presence of triplet-triplet reactions*

Consider a triplet excited state that undergoes ground-state quenching and triplet-triplet reaction simultaneously.





The decay of \*S after pulsed excitation does not follow first-order kinetics:  $-d[*S]/dt = K[*S] + k_1[*S]^2$ , where  $K = (k_0 + k_q[S])$ .

*Ref. 83A102.*  $K$  and  $k_1$  were evaluated by a best-fit procedure from the decay curves of the optical absorption of \*S using Eq. (40), obtained from the solution of the differential equation above. Conversion of absorbances to concentrations was effected by using the following relationships:  $[*S]_0 = (A_0 - A_b)/\epsilon(*S)$  and  $[*S]_t = (A_t - A_b)/\epsilon(*S)$ , where  $\epsilon(*S)$  is the molar absorptivity of \*S at the monitoring wavelength, and  $A_b$ ,  $A_0$  and  $A_t$  are the optical absorbances before the flash, just after the flash, and at time  $t$  after the flash, respectively.  $k_q$  was then obtained as the slope of the linear plot of  $K$  vs  $[S]$ .

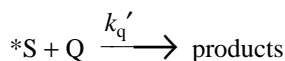
$$[*S]_t = \frac{(K/k_1)}{\left[ \frac{K}{k_1[*S]_0} + 1 \right] \exp(Kt) - 1} \quad (40)$$

*Ref. 60E006.* For similar systems,  $K$  was evaluated by means of Eq. (41), where  $\epsilon(S)$  is the molar absorptivity at the monitoring wavelength,  $l$  is the optical pathlength, and  $\epsilon(*S)$ ,  $A_b$ ,  $A_0$ , and  $A_t$  have the same meaning as above.

$$\frac{d\{\ln [(A_0 - A_b)/(A_t - A_b)]\}}{dt} = K + \left[ \frac{(k_1 - k_q)(A_t - A_b)}{[\epsilon(*S) - \epsilon(S)]l} \right] \quad (41)$$

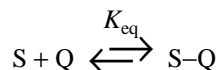
The value of the derivative [left side of Eq. (41)] was determined as the tangent to the plot of  $(A_0 - A_b)/(A_t - A_b)$  vs  $t$ , and  $K$  as the intercept of the plot of the derivative vs  $(A_t - A_b)$ .

*Ref. 60A002.* The same treatment as above was applied to the quenching of \*S by Q. Now,  $K = k_0 + k_q[S] + k_q'[Q]$  in Eq. (41);  $k_q'$  was evaluated from the plot of  $K$  vs  $[Q]$  at constant  $[S]$ .

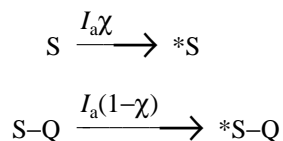


#### *Mech. [11] Static quenching*

Static quenching is a nondynamical process that results from the excitation of ground-state adducts between S and Q; static quenching may occur simultaneously with the dynamic quenching reaction, particularly when S and Q are ions of opposite sign.



When the emission from \*S (and \*S-Q) is measured under steady-state conditions, the light absorption step of Sec. 2.2 must be replaced with the following reactions, where  $I_a$  is the intensity of light absorbed by all the various S species, and  $\chi$  is the fraction of the light absorbed by uncomplexed S;  $\chi = (1 + K_{eq}[Q])^{-1}$  if S and S-Q have the same molar absorptivity at the exciting wavelength.



If it is assumed that  $K_{eq} = k_d/k_{-d}$ , the general steady-state treatment leads to expressions for the dependence of the emission intensity on  $[Q]$ : Eq. (42) for irreversible quenching (reaction (5) in Sec. 2.3), and Eq. (43) for reversible quenching (reaction (6) in Sec. 2.3).

$$I_t^0/I_t = 1 + (K_{SV} + K_{eq})[Q] + K_{SV}K_{eq}[Q]^2 \quad (42)$$

$$\frac{I_l^0}{I_l} = \frac{1 + (K_{SV} + K_{eq})[Q] + K_{SV}K_{eq}[Q]^2}{1 + (1 + \gamma) \left[ \frac{k_d[Q]}{k_{-d} + k_{de}} \right] + \gamma \left[ \frac{(k_0 + k_d[Q])K_{eq}[Q]}{k_{-d} + k_{de}} \right]} \quad (43)$$

Equation (42) is a quadratic equation which shows positive deviation from linearity when  $I_l^0/I_l$  is plotted against  $[Q]$ . Equation (43), on the other hand, tends toward a limiting value at high  $[Q]$ :  $I_l^0/I_l$  (lim) =  $k_{de}/k_0\gamma$ . Equation (43) reduces to Eq. (42) whenever the denominator of 43 is close to unity, in particular when  $(k_{-d} + k_{de}) \gg k_d[Q]$  and  $k_{de} \gg k_0$ . If one assumes that  $k_{rd}' = k_{rd}$ , the condition that  $k_{de} \gg k_0$  implies that the quantum yield of emission from  $*S-Q$  is much smaller than that from  $*S$ .

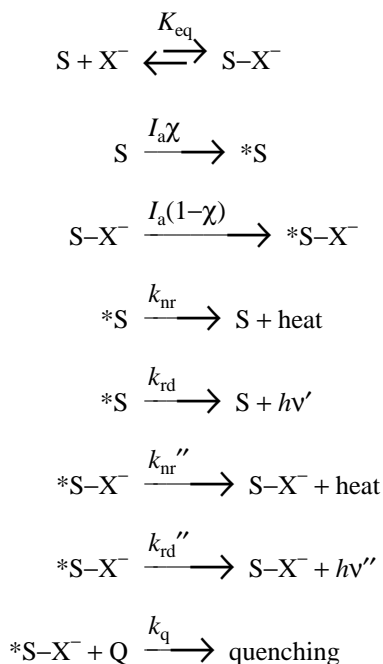
In pulsed excitation experiments, ground-state complexation between S and Q affects  $[*S]$  and  $[*S-Q]$  at  $t = 0$  after the flash, but not their decay kinetics. Then, only the "dynamic" part of the quenching, which generally is monoexponential and exhibits a linear S-V plot, is monitored.

*Refs. 80E669 and 81A250.*  $k_q$  was obtained from steady-state emission intensity measurements by assuming that  $I_l^0/I_l$  follows Eq. (42). In the first paper, however, the S-V plot has a negative deviation from linearity. In the latter paper, a value of  $K_{eq}$ , obtained from the Debye-Smoluchowski and Eigen equations, was used in the best-fit procedure to evaluate  $K_{SV}$ .

*Ref. 85E375.* A biexponential decay of the emission after pulsed excitation was observed in the presence of static quenching. The values of  $k_d$ ,  $k_{-d}$ , and  $k_{de}$  were obtained through a best-fit procedure from  $m_1$  and  $m_2$  values at two different  $[Q]$ , by assuming that  $k_{rd}' = k_{rd}$ ,  $k_{nr}' = k_{nr}$ , and  $k_{rx}' = k_{rx}$ . The value of  $k_q$  reported in this compilation was calculated by us using the values of  $k_d$ ,  $k_{-d}$ , and  $k_{de}$  quoted in this paper.

#### *Mech. [12] Ion-pairing of the substrate*

*Ref. 86F346.* For the system where the substrate is  $\text{Ru}(\text{bpy})_3^{2+}$  and the quencher is  $\text{MV}^{2+}$ , it has been found that the quenching reaction is affected by both the nature and the concentration of added halide ions ( $X^- = \text{Cl}^-, \text{I}^-$ ). This behavior was attributed to the presence of ion-pairs between S and  $X^-$ , their excitation, and subsequent quenching. The following mechanism was assumed:



The quenching of "free"  $*S$  by Q, and ion-pairing between Q and  $X^-$  were ignored. A steady-state treatment, in which it was assumed that  $\epsilon(\text{S}) = \epsilon(\text{S-X}^-)$  at the excitation wavelength,  $k_{rd} = k_{rd}''$ , and  $k_{nr} = k_{nr}''$ , leads to Eq. (44).

$$\frac{I_l^0}{I_l} = 1 + \frac{K_{eq}[X^-]K_{SV}[Q]}{1 + K_{eq}[X^-] + K_{SV}[Q]} \quad (44)$$

In this treatment,  $[X^-]$  was taken to be equal to  $[X^-]_0$ , the concentration of  $X^-$  in the initially prepared solution, inasmuch as  $[S] < [X^-]_0$ . Equation (44) is converted easily to Eq. (45).

$$Y = \frac{[Q]}{\left[ \frac{I_l^0}{I_l} - 1 \right]} = \left[ \frac{1}{K_{SV}} \right] + \left[ \frac{1 + K_{SV}[Q]}{K_{eq}K_{SV}} \right] \left[ \frac{1}{[X^-]} \right] \quad (45)$$

A linear plot of  $Y$  vs  $1/[X^-]$  was obtained at constant  $[Q]$ ;  $K_{SV}$  was calculated directly from the intercept of this plot. It is worth noting that changes in  $[X^-]$  also caused changes in the ionic strength of the solution; this fact was not considered in the paper.

### 7.1. References to Notes on the Tables

- 60A002 The quenching of triplet states of anthracene and porphyrins by heavy metal ions.  
Linschitz, H.; Pekkarinen, L., *J. Am. Chem. Soc.* **82**: 2411-6 (1960)
- 60E006 Studies on metastable states of porphyrins. II. Spectra and decay kinetics of tetraphenylporphine, zinc tetraphenylporphine and bacteriochlorophyll.  
Pekkarinen, L.; Linschitz, H., *J. Am. Chem. Soc.* **82**: 2407-11 (1960)
- 74E519 Fluorescence enhancement of  $Eu^{3+}$  by  $Tb^{3+}$  in dimethylsulfoxide (DMSO).  
Chrysochoos, J., *J. Lumin.* **9**: 79-93 (1974)
- 756452 Pentavalent uranium, a quencher of the excited state of uranyl in solution.  
Bulgakov, R.G.; Kazakov, V.P.; Lotnik, S.V., *High Energy Chem. (Engl. Transl.)* **9**: 493-4 (1975) Translated from: *Khim. Vys. Energ.* **9**: 555-6 (1975)
- 78A058 Photoinduced electron transfer reactions between tris(2,2'-bipyridine)osmium(II) and various acidopentaamminecobalt(III) complexes.  
Finkenberg, E.; Fisher, P.; Huang, S.-M.Y.; Gafney, H.D., *J. Phys. Chem.* **82**: 526-31 (1978)
- 79A220 Kinetics of triplet oxidation of metalloporphyrin compounds to their corresponding radical cations.  
Potter, W.; Levin, G., *Photochem. Photobiol.* **30**: 225-31 (1979)
- 79E349 Exciplex formation from transition-metal complexes. Luminescent nonpolar exciplexes from palladium(II) porphyrin triplets and N,N-dimethylaniline.  
Mercer-Smith, J.A.; Sutcliffe, C.R.; Schmehl, R.H.; Whitten, D.G., *J. Am. Chem. Soc.* **101**: 3995-7 (1979)
- 80A023 Photochemical ionogenesis in solutions of zinc octaethyl porphyrin.  
Ballard, S.G.; Mauzerall, D.C., *J. Chem. Phys.* **72**: 933-47 (1980)
- 80E224 An electrochemical study of quenching reactions of polypyridine complexes of Ru(II) and Os(II) in excited states.  
Ohsawa, Y.; Saji, T.; Aoyagui, S., *J. Electroanal. Chem. Interfacial Electrochem.* **106**: 327-38 (1980)
- 80E412 Singlet energy transfer from the charge transfer excited state of tris(2,2'-bipyridine)ruthenium(II).  
Mandal, K.; Pearson, T.D.L.; Demas, J.N., *J. Chem. Phys.* **73**: 2507-9 (1980)
- 80E669 Attempted photoproduction of hydrogen using sulphophthalocyanines as chromophores for three-component systems.  
Harriman, A.; Richoux, M.-C., *J. Chem. Soc., Faraday Trans. 2* **76**: 1618-26 (1980)
- 80F058 Photochemical reduction of some carboxylatopentaamminecobalt(III) complexes by tris(bipyridine)ruthenium(II). Evidence for cage recombination reactions.  
Boettcher, W.; Haim, A., *J. Am. Chem. Soc.* **102**: 1564-9 (1980)
- 80F228 Photoreacemization of  $Ru(bipyridine)_3^{2+}$ .  
Porter, G.B.; Sparks, R.H., *J. Photochem.* **13**: 123-31 (1980)
- 81A139 Kinetic studies of photoinduced methyl viologen reduction with ruthenium complexes and hydrogen evolution from water by hydrogenase.  
Okura, I.; Kim-Thuan, N., *J. Chem. Soc., Faraday Trans. 1* **77**: 1411-5 (1981)
- 81A250 Optically induced electron transfer within ion pairs. The  $Os(5-Cl-phen)_3^{2+}$ - $Fe(CN)_6^{4-}$  system.  
Rybak, W.; Haim, A.; Netzel, T.L.; Sutin, N., *J. Phys. Chem.* **85**: 2856-60 (1981)

- 81E458 Photophysics and photochemistry of polypyridyl complexes of chromium(III).  
Serpone, N.; Jamieson, M.A.; Sriram, R.; Hoffman, M.Z., *Inorg. Chem.* **20**: 3983-8 (1981)
- 82E073 Excited state processes for aqueous  $\text{Rh}(\text{NH}_3)_5\text{Cl}^{2+}$  and  $\text{Rh}(\text{NH}_3)_5\text{Br}^{2+}$ .  
Larson, M.; Maেকে, H.; Rumfeldt, R.C.; Adamson, A.W., *Inorg. Chim. Acta* **57**: 229-35 (1982)
- 82E636 Kinetic study of triplet complexes of porphyrins with quinones.  
Kapinus, E.I.; Staryi, V.P.; Dilung, I.I., *Theor. Exp. Chem.* **18**: 402-9 (1982) Translated from: *Teor. Eksp. Khim.* **18**: 450-8 (1982)
- 82F065 An analysis of the mechanistic pathways in the reversible photoinduced reactions between  $^*\text{Ru}(\text{bpy})_3^{2+}$  and  $\text{Co}(\text{phen})_3^{3+}$  by flash photolysis techniques.  
Krist, K.; Gafney, H.D., *J. Phys. Chem.* **86**: 951-8 (1982)
- 83A101 Exciplex processes involving trans naphthylethylenes. Implications of ground-state conformeric equilibria.  
Wisniewski-Knittel, T.; Sofer, I.; Das, P.K., *J. Phys. Chem.* **87**: 1745-52 (1983)
- 83A102 Mechanism of porphyrin ion production from the triplet state of magnesium octaethylporphyrin.  
Smalley, J.F.; Feldberg, S.W.; Brunschwig, B.S., *J. Phys. Chem.* **87**: 1757-65 (1983)
- 83A333 Reduction of macrocyclic cobalt(III) complex photosensitized by tris(2,2'-bipyridine)ruthenium(II).  
Kurimura, Y.; Endo, E., *Bull. Chem. Soc. Jpn.* **56**: 3835-6 (1983)
- 84A141 Reaction dynamics and hydroxide ion quenching of rhodium(III) ligand field excited states: Photoreactions of  $\text{Rh}(\text{NH}_3)_5\text{I}^{2+}$ .  
Frink, M.E.; Magde, D.; Sexton, D.; Ford, P.C., *Inorg. Chem.* **23**: 1238-40, 2728 (1984)
- 84E308 Formation of exciplexes during deactivation of the triplet state of magnesium phthalocyanine by nitroxide radicals.  
Degtyarev, L.S.; Kapinus, E.I.; Skuridin, E.Yu., *High Energy Chem.* **18**: 43-5 (1984) Translated from: *Khim. Vys. Energ.* **18**: 56-9 (1984)
- 84F351 Tris(bipyridyl)ruthenium(II)-photosensitized reaction of 1-benzyl-1,4-dihydronicotinamide with benzyl bromide.  
Hironaka, K.; Fukuzumi, S.; Tanaka, T., *J. Chem. Soc., Perkin Trans. 2* : 1705-9 (1984)
- 85A013 Laser photolysis studies on the electron-transfer reaction from the photoexcited triplet state of chloroindium(III) tetraphenylporphyrin to methylviologen in methanol solutions.  
Hoshino, M.; Seki, H.; Shizuka, H., *J. Phys. Chem.* **89**: 470-4 (1985)
- 85E375 Photoinduced electron transfer within ion pairs. Direct measure of the intramolecular electron-transfer quenching constant.  
Ballardini, R.; Gandolfi, M.T.; Balzani, V., *Chem. Phys. Lett.* **119**: 459-62 (1985)
- 85F328 Metalloporphyrin-sensitized photoredox reactions: Mechanistic studies on the role of axial ligands on photoreactivity.  
Inoue, H.; Chandrasekaran, K.; Whitten, D.G., *J. Photochem.* **30**: 269-84 (1985)
- 85F395 Photosensitized isomerization of norbornadiene to quadricyclane with (arylphosphine)copper(I) halides.  
Fife, D.J.; Moore, W.M.; Morse, K.W., *J. Am. Chem. Soc.* **107**: 7077-83 (1985)
- 86A158 Charge-transfer sensitization of the valence photoisomerization of norbornadiene to quadricyclane by an orthometalated transition-metal complex.  
Grutsch, P.A.; Kutal, C., *J. Am. Chem. Soc.* **108**: 3108-10 (1986)
- 86E555 Phosphorescent 8-quinolinol metal chelates. Excited-state properties and redox behavior.  
Ballardini, R.; Varani, G.; Indelli, M.T.; Scandola, F., *Inorg. Chem.* **25**: 3858-65 (1986)
- 86E677 Study of self-quenching by steady state emission measurements.  
Favaro, G., *J. Photochem.* **35**: 375-9 (1986)
- 86F346 Solvation effects on photochemically-induced electron transfer from tris(bipyridyl)ruthenium to methylviologen.  
Ochiai, E.-I.; Shaffer, D.I.; Wampler, D.L.; Schettler, P.D., Jr., *Transition Met. Chem. (Weinheim, Ger.)* **11**: 241-6 (1986)

## 8. Lists of Abbreviations and Symbols

### LIGANDS

acac	Acetylacetonate ion
AMcapten	1-Methyl-8-amino-6,13,19-triaza-3,10,16-trithiabicyclo[6.6.6]eicosane
AMMEsar	1-Amino-8-methyl-3,6,10,13,16,19-hexaazabicyclo[6.6.6]eicosane
AMMEsarH	1-Amino-8-methyl-3,6,10,13,16,19-hexaazabicyclo[6.6.6]eicosane, protonated
13-At	1,4,7,10-Tetraazacyclotrideca-10-13-dienate ion, Fig. 1
AZAcapten	1-Methyl-6,8,13,19-tetraaza-3,10,16-trithiabicyclo[6.6.6]eicosane
AZAMEsar	8-Methyl-1,3,6,10,13,16,19-heptaazabicyclo[6.6.6]eicosane
benzo-15-crown-5	2,3-Benzo-1,4,7,10,13-pentaoxapentadeca-2-ene
bpy	2,2'-Bipyridine
-bpy	2,2'-Bipyridine (as monodentate ligand)
C <sup>3</sup> ,N'-bpy	2,2'-Bipyridyl-C <sup>3</sup> ,N'
5-Brphen	5-Bromo-1,10-phenanthroline
4,4'-Bu <sub>2</sub> bpy	4,4'-Bis( <i>tert</i> -butyl)-2,2'-bipyridine
(BUG) <sub>2</sub> bpy	2,2'-Bipyridine with polymeric side chains, Fig. 2
bzac	1-Phenyl-1,3-butanedionate ion
4,4'-Cl <sub>2</sub> bpy	4,4'-Dichloro-2,2'-bipyridine
CLNOSar	1-Chloro-8-nitro-3,6,10,13,16,19-hexaazabicyclo[6.6.6]eicosane
CLOHsar	1-Chloro-8-hydroxy-3,6,10,13,16,19-hexaazabicyclo[6.6.6]eicosane
5-Clphen	5-Chloro-1,10-phenanthroline
CLsar	1-Chloro-3,6,10,13,16,19-hexaazabicyclo[6.6.6]eicosane
CMMEabsar	1-Chloromethyl-8-methyl-3,6,10,13,15,18-hexaazabicyclo[6.6.5]nonadecane
4,4'-(COO) <sub>2</sub> bpy	2,2'-Bipyridine-4,4'-dicarboxylate ion
4,4'-(COObz) <sub>2</sub> bpy	2,2'-Bipyridine-4,4'-dicarboxylic acid, dibenzyl ester
4,4'-(COOchl) <sub>2</sub> bpy	2,2'-Bipyridine-4,4'-dicarboxylic acid, di(3β-cholestyl) ester
4,4'-(COOcyc) <sub>2</sub> bpy	2,2'-Bipyridine-4,4'-dicarboxylic acid, dicyclohexyl ester
4,4'-(COOdec) <sub>2</sub> bpy	2,2'-Bipyridine-4,4'-dicarboxylic acid, di(1-decahydronaphthyl) ester
4,4'-(COOet) <sub>2</sub> bpy	2,2'-Bipyridine-4,4'-dicarboxylic acid, diethyl ester
4,4'-(COOH) <sub>2</sub> bpy	2,2'-Bipyridine-4,4'-dicarboxylic acid
4,4'-(COOnap) <sub>2</sub> bpy	2,2'-Bipyridine-4,4'-dicarboxylic acid, di(2-naphthyl) ester
4,4'-(COOpr) <sub>2</sub> bpy	2,2'-Bipyridine-4,4'-dicarboxylic acid, di(2-propyl) ester
crypt	4,7,13,16,21-Pentaoxa-1,10-diazabicyclo[8.8.5]tricosane
cyclam	1,4,8,11-Tetraazacyclotetradecane
dbm	1,3-Diphenyl-1,3-propanedionate ion
diAMchar	1,12-Diamino-3,10,14,21,24,31-hexaazapentacyclo[10.10.10. <sup>4,9</sup> .0 <sup>15,20</sup> .0 <sup>25,30</sup> ]dotriacontane
diAMsar	1,8-Diamino-3,6,10,13,16,19-hexaazabicyclo[6.6.6]eicosane
diAMsarH <sub>2</sub>	1,8-Diamino-3,6,10,13,16,19-hexaazabicyclo[6.6.6]eicosane, diprotonated
diAZAchar	1,3,10,12,14,21,24,31-Ocataazapentacyclo[10.10.10. <sup>4,9</sup> .0 <sup>15,20</sup> .0 <sup>25,30</sup> ]dotriacontane
diCLsar	1,8-Dichloro-3,6,10,13,16,19-hexaazabicyclo[6.6.6]eicosane
diNOSar	1,8-Dinitro-3,6,10,13,16,19-hexaazabicyclo[6.6.6]eicosane
DMF	<i>N,N</i> -Dimethylformamide
DMG	Dimethylglyoximate ion
DMSO	Dimethylsulfoxide
Do <sub>2</sub> Ca <sub>2</sub> bpy	1,1'-Didodecyl-2,2'-bipyridine-4,4'-dicarboxamide
EDTA	Ethylenediaminetetraacetate ion
EFMEoxosar-H	1-Carbethoxy-2-oxo-8-methyl-3,6,10,13,16,19-hexaazabicyclo[6.6.6]eicosane, deprotonated form
en	Ethylenediamine
etioporphyrin I	2,7,12,17-Tetraethyl-3,8,13,18-tetramethylporphyrin
4-(Et <sub>3</sub> P)bpy	2,2'-Bipyridine-4-(triethylphosphonio) cation
gly	Glycinate ion
C <sup>3</sup> ,N'-Hbpy	2,2'-Bipyridyl-C <sup>3</sup> ,N', protonated
HEDTA	Monohydrogen ethylenediaminetetraacetate ion
hfac	1,1,1,5,5,5-Hexafluoro-2,4-pentanedionate ion
HYMEoxosar-H	2-Oxo-8-methyl-3,6,10,13,16,19-hexaazabicyclo[6.6.6]eicosane, deprotonated form
3,3'-Me <sub>2</sub> bpy	3,3'-Dimethyl-2,2'-bipyridine
4,4'-Me <sub>2</sub> bpy	4,4'-Dimethyl-2,2'-bipyridine
Me <sub>6</sub> cycladiene	5,7,7,12,14,14-Hexamethyl-1,4,8,11-tetraazacyclotetradeca-4,11-diene
Me <sub>6</sub> cyclam	5,7,7,12,14,14-Hexamethyl-1,4,8,11-tetraazacyclotetradecane
Me <sub>2</sub> dibenzoH <sub>2</sub> phen	6,7-Dihydro-5,8-dimethyldibenzo[ <i>b,j</i> ]1,10-phenanthroline (DMCH)
MENOSar	1-Methyl-8-nitro-3,6,10,13,16,19-hexaazabicyclo[6.6.6]eicosane
5-Mephen	5-Methyl-1,10-phenanthroline
2,9-Me <sub>2</sub> phen	2,9-Dimethyl-1,10-phenanthroline

4,7-Me <sub>2</sub> phen	4,7-Dimethyl-1,10-phenanthroline
5,6-Me <sub>2</sub> phen	5,6-Dimethyl-1,10-phenanthroline
3,4,7,8-Me <sub>4</sub> phen	3,4,7,8-Tetramethyl-1,10-phenanthroline
3,5,6,8-Me <sub>4</sub> phen	3,5,6,8-Tetramethyl-1,10-phenanthroline
MePh <sub>2</sub> P	Methyldiphenylphosphine
mesoporphyrin IX	7,12-Diethyl-3,8,13,17-tetramethylporphyrin-2,18-dipropionic acid
<i>N</i> -Mevio	<i>N</i> -Methyl-4-(4-pyridyl)pyridinium cation
5-(NH <sub>2</sub> )phen	5-Amino-1,10-phenanthroline
2-(NO <sub>2</sub> )benz	2-Nitrobenzoate ion
4-(NO <sub>2</sub> )benz	4-Nitrobenzoate ion
4-(NO <sub>2</sub> )bpy	4-Nitro-2,2'-bipyridine
5-(NO <sub>2</sub> )phen	5-Nitro-1,10-phenanthroline
NTA	Nitritotriacetate ion
OEP	2,3,7,8,12,13,17,18-Octaethylporphyrin
pdo	1,3-Propanedionate ion
4,4'-Ph <sub>2</sub> bpy	4,4'-Diphenyl-2,2'-bipyridine
phen	1,10-Phenanthroline
5-Phphen	5-Phenyl-1,10-phenanthroline
2,9-Ph <sub>2</sub> phen	2,9-Diphenyl-1,10-phenanthroline
4,7-Ph <sub>2</sub> phen	4,7-Diphenyl-1,10-phenanthroline
4,7-(PhSO <sub>3</sub> ) <sub>2</sub> phen	1,10-Phenanthroline-4,7-di(phenyl-4-sulfonate) ion
py	Pyridine
sar	3,6,10,13,16,19-Hexaazabicyclo[6.6.6]eicosane
sep	1,3,6,8,10,13,16,19-Octaazabicyclo[6.6.6]eicosane
4,4'-(SO <sub>3</sub> ) <sub>2</sub> bpy	2,2'-Bipyridine-4,4'-disulfonate ion
TEOA	Triethanolamine
terpy	2,2',2''-Terpyridine
tfac	1,1,1-Trifluoro-2,4-pentanedionate ion
tfbzac	1-Phenyl-4,4,4-trifluoro-1,3-butanedionate ion
thd	2,2,6,6-Tetramethyl-3,5-heptanedionate ion
TMePyP	5,10,15,20-Tetrakis(1-methylpyridinium-4-yl)porphyrin
TPP	5,10,15,20-Tetraphenylporphyrin
TPTZ	2,4,6-Tris(2-pyridyl)-1,3,5-triazine
tta	1-Thienyl-4,4,4-trifluoro-1,3-butanedionate ion
uroporphyrin I	Porphyrin-2,7,12,17-tetraacetic-3,8,13,18-tetrapropionic acid

## ORGANIC QUENCHERS

bpy	2,2'-Bipyridine
bpy <sup>2+</sup>	2,2'-Bipyridinium dication (in <i>N,N'</i> -disubstituted derivatives)
bpyH <sup>+</sup>	2,2'-Bipyridine, monoprotonated
bpyH <sub>2</sub> <sup>2+</sup>	2,2'-Bipyridine, diprotonated
β-CD	β-Cyclodextrin
CDTA	<i>trans</i> -1,2-Diaminocyclohexane- <i>N,N,N',N'</i> -tetraacetic acid
DDT	2,2-Bis(4-chlorophenyl)-1,1,1-trichloroethane
DMSO	Dimethylsulfoxide
DQ <sup>2+</sup>	<i>N,N'</i> -Ethylene-2,2'-bipyridinium dication (Diquat)
EDTA	Ethylenediaminetetraacetic acid
H-3-pyl	Pyridinium-3-yl cation radical
H-4-pyl	Pyridinium-4-yl cation radical
Me-2-pyl	<i>N</i> -Methylpyridinium-2-yl cation radical
Me-3-pyl	<i>N</i> -Methylpyridinium-3-yl cation radical
Me-4-pyl	<i>N</i> -Methylpyridinium-4-yl cation radical
MV <sup>2+</sup>	<i>N,N'</i> -Dimethyl-4,4'-bipyridinium dication (methylviologen, Paraquat)
OrgQue1	see Fig. 3
OrgQue2	see Fig. 3
OrgQue3	see Fig. 3
OrgQue4	see Fig. 3
OrgQue5	see Fig. 3
OrgQue6	2,1,3-Benzothiadiazole-4,7-dicarbonitrile, Fig. 4
OrgQue7	1,1'-Bis(phenylmethyl)-3,3'-dicarboxamide-1,1',4,4'-tetrahydro-4,4'-bipyridine, Fig. 5
OrgQue8	see Fig. 6
OrgQue9	see Fig. 6
OrgQue10	see Fig. 6
OrgQue11	see Fig. 7a
OrgQue12	see Fig. 7b

OrgQue13	2,2,6,6-Tetramethyl-4-oxopiperidine-1-oxyl radical, Fig. 8a
OrgQue14	2,2,6,6-Tetramethylpiperidine-1-oxyl radical, Fig. 8b
phen <sup>2+</sup>	1,10-Phenanthroline dication (in <i>N,N'</i> -disubstituted derivatives)
phenH <sup>+</sup>	1,10-Phenanthroline, monoprotonated
phenH <sub>2</sub> <sup>2+</sup>	1,10-Phenanthroline, diprotonated
Poly-2,4-ionene	Poly[(dimethylimino)-1,4-butanediyl(dimethylimino)-1,2-ethanediyl dication], Fig. 9
PolyPTZ	Polymeric phenothiazine, see Fig. 10
PolyVio1	Polymeric viologen, see Fig. 11
PolyVio2	Polymeric viologen, see Fig. 12
PolyVio3	Polymeric viologen, see Fig. 13
PolyVio4	Polymeric viologen, see Fig. 13
PolyVio5	Polymeric viologen, see Fig. 13
PolyVio6	Polymeric viologen, see Fig. 13
PolyVio7	Polymeric viologen, see Fig. 13
PolyVio8	Polymeric viologen, see Fig. 13
PolyVio9	Polymeric viologen, see Fig. 13
PolyVio10	Polymeric viologen, see Fig. 14
PolyVio11	Polymeric viologen, see Fig. 15
PolyVio12	Polymeric viologen, see Fig. 16
PolyVio13	Polymeric viologen, see Fig. 16
PolyVio14	Polymeric viologen, see Fig. 17
py	Pyridine
py <sup>+</sup>	Pyridinium cation (in <i>N</i> -substituted derivatives)
pyH <sup>+</sup>	Pyridine, protonated
sydnone	1,2,3-Oxadiazol-5-one, Fig. 18 (in mono- and disubstituted derivatives)
Triton X-100	C <sub>8</sub> H <sub>17</sub> C <sub>6</sub> H <sub>4</sub> (OCH <sub>2</sub> CH <sub>2</sub> ) <sub>x</sub> OH (x = 9 or 10)
vio	4,4'-Bipyridine (viologen)
vio <sup>+</sup>	4-(4-Pyridyl)pyridinium cation (in <i>N</i> -monosubstituted derivatives)
vio <sup>2+</sup>	4,4'-Bipyridinium dication (in <i>N,N'</i> -disubstituted derivatives)
vioH <sup>+</sup>	4,4'-Bipyridine, monoprotonated
vioH <sup>2+</sup>	4-(4-Pyridyl)pyridinium cation, protonated (in <i>N</i> -mono-substituted derivatives)
vioH <sub>2</sub> <sup>2+</sup>	4,4'-Bipyridine, diprotonated

## OTHER MATERIALS

ACbuf	Acetate buffer
AN	Acetonitrile
AQN	Poly[imino-2-(dimethylamino)hexamethylene-1-oxo], Fig. 19
BHDC	Benzyltrimethyl- <i>n</i> -hexadecylammonium chloride
BObuf	Borate buffer
BRbuf	Britton-Robinson buffer (0.008 mol/L acetate, 0.008 mol/L phosphate, 0.008 mol/L borate)
<i>n</i> -BuOH	1-Butanol
<i>t</i> -BuOH	<i>tert</i> -Butyl alcohol
BuN	<i>iso</i> -Butyronitrile
CABuf	Carbonate buffer
6CB	Cyanohexylbiphenyl
β-CD	β-Cyclodextrin
CMC	critical micelle concentration
CTAB	Cetyltrimethylammonium bromide
CTAC	Cetyltrimethylammonium chloride
DMA	<i>N,N</i> -Dimethylacetamide
DMF	<i>N,N</i> -Dimethylformamide
DMSO	Dimethylsulfoxide
dTBP	Tributylphosphate (perdeuterated)
EDTA	Ethylenediaminetetraacetic acid
EtMO	<i>N</i> -Ethylmorpholine
EtOH	Ethanol
FA	Formamide
HAc	Acetic acid
HSEtOH	Mercaptoethanol
IMIDbuf	Imidazole buffer
MeCH	Methylcyclohexane
MeOH	Methanol
Me <sub>2</sub> SO <sub>4</sub>	Sulfuric acid, dimethyl ester
MF	<i>N</i> -Methylformamide
MP	<i>N</i> -Methylpropionamide

NaAc	Sodium acetate
NTA	Nitrilotriacetate ion
Pbuf	Phosphate buffer
PHTHbuf	Phthalate buffer
PMA	Poly(methacrylic acid)
polybrene	Poly[(dimethyliminio)-1,3-propanediyl(dimethyliminio)-1,6-hexadiyl dication], Fig. 20; concentration based on the ionic charge
PPh <sub>3</sub>	Triphenylphosphine
1-PrOH	1-Propanol
2-PrOH	2-Propanol
PVA	Poly(vinylalcohol)
PVS	Poly(vinylsulfate)
py	Pyridine
PYbuf	Pyridine buffer
SLS	Sodium lauryl sulfate
TBAB	Tetrabutylammonium bromide
TBAC	Tetrabutylammonium chloride
TBAF	Tetrabutylammonium hexafluorophosphate
TBAP	Tetrabutylammonium perchlorate
TBAS	Tetrabutylammonium trifluoromethylsulfate
TBP	Tributylphosphate
TEAC	Tetraethylammonium chloride
TEAP	Tetraethylammonium perchlorate
TEOA	Triethanolamine
THF	Tetrahydrofuran
TMAC	Tetramethylammonium chloride
TMP	Trimethylphosphate
TOAB	Tetraoctylammonium bromide
TPeAC	Tetrapentylammonium chloride
TPrAB	Tetrapropylammonium bromide
TPrAC	Tetrapropylammonium chloride
TRbuf	Tris buffer

## OTHER ABBREVIATIONS AND SYMBOLS

(calc)	calculated from $\tau$ and $K_{SV}$ or from rate constants for specific steps
(corr)	corrected for diffusional effects
$E_a$	activation energy
EQ	quenching of an higher-energy state
estd	estimated
$f$	fraction of quenching acts that yield electron-transfer products in the bulk solution
$k_{dif}$	diffusion rate constant ( $L mol^{-1} s^{-1}$ )
$k_{obs}$	experimentally observed rate constant
$k_q$	quenching rate constant
$K_{SV}^{\ddagger}$	Stern-Volmer constant
$K_{SV}$	Stern-Volmer constant from lifetime measurements
L	ligand
$p_Q$	partial pressure of gaseous Q in equilibrium with the solution
$p_{app}$	applied pressure
Q	quencher
S	substrate
*S	excited state of the substrate involved in quenching
SQ	static quenching
S-V	Stern-Volmer
TT	triplet-triplet annihilation
$\Delta G^*$	free energy of activation
$\Delta H^*$	enthalpy of activation
$\Delta S^*$	entropy of activation
$\Delta V^*$	volume of activation
$\eta^*$	efficiency of population of the quenched excited state
$\mu$	ionic strength (mol/L)
$\tau_{0,dir}$	lifetime in the absence of quencher, air-free solution
$\tau_{0,und}$	lifetime in the absence of quencher, air-equilibrated solution
$\tau_0$	lifetime in the absence of quencher, solution of unknown $O_2$ content
$\phi$	quantum yield of formation of the quenched excited state